



Published in final edited form as:

Hum Genet. 2012 February ; 131(2): 235–250. doi:10.1007/s00439-011-1064-z.

The Cell-Adhesion Gene *PVRL3* is Associated with Congenital Ocular Defects

Salil A. Lachke^{1,2,†}, Anne W. Higgins^{3,†,¶}, Maiko Inagaki⁴, Irfan Saadi^{1,§}, Qiongchao Xi¹, Michelle Long³, Bradley J. Quade³, Michael E. Talkowski⁵, James F. Gusella⁵, Atsuko Fujimoto⁶, Michael L. Robinson⁷, Ying Yang⁸, Quynh T. Duong⁹, Irit Shapira¹⁰, Benny Motro¹⁰, Jun Miyoshi¹¹, Yoshimi Takai¹², Cynthia C. Morton³, and Richard L. Maas^{1,*}

¹Division of Genetics, Department of Medicine, Brigham and Women's Hospital, Harvard Medical School, Boston, MA 02115 USA

²Department of Biological Sciences, University of Delaware, Newark DE 19716 USA

³Departments of Obstetrics, Gynecology and Reproductive Biology and of Pathology, Brigham and Women's Hospital, Harvard Medical School, Boston, MA 02115 USA

⁴Radiation Research Center for Frontier Science Research, Institute for Radiation Biology and Medicine, Hiroshima University, 1-2-3 Kasumi, Minami-ku, Hiroshima 734-8553 Japan

⁵Molecular Neurogenetics Unit, Center for Human Genetic Research, Massachusetts General Hospital and Department of Genetics, Harvard Medical School, Boston, MA 02114 USA

⁶Department of Pediatrics, Keck School of Medicine, University of Southern California Medical Center, Los Angeles, CA 90033 USA

⁷Department of Zoology, Miami University, Oxford, OH 45056 USA

⁸Center for Human and Molecular Genetics, Columbus Children's Research Institute, Columbus, OH 43205 USA

⁹The Ohio State University College of Optometry, Columbus, OH 43210 USA

¹⁰The Mina and Everard Goodman Faculty of Life Sciences, Bar-Ilan University, Ramat-Gan 52900 Israel

¹¹Department of Molecular Biology, Osaka Medical Center for Cancer and Cardiovascular Diseases, Osaka 537-8511 Japan

¹²Division of Molecular and Cellular Biology, Kobe University Graduate School of Medicine, Kobe 650-0017 Japan

Abstract

We describe a male patient (patient DGAP113) with a balanced translocation, 46,XY,t(1;3)(q31.3;q13.13), severe bilateral congenital cataracts, CNS abnormalities and mild developmental delay. Fluorescence *in situ* hybridization (FISH) and suppression PCR demonstrated that the

*Correspondence: Richard Maas, M.D., Ph.D., maas@genetics.med.harvard.edu Phone: 617-525-4706; Fax: 617-525-4751.

†These authors contributed equally to this work

¶Present Address: Departments of Hospital Laboratories and Pathology, UMass Memorial Medical Center and UMass Medical School, Worcester, MA 01605 USA

§Present Address: Department of Anatomy and Cell Biology, KU Medical Center, Kansas City, KS 66160 USA

SUPPLEMENTAL DATA

Supplemental data include five figures and one table and can be found with this article online.

The authors declare no conflicts of interest.

chromosome 3 breakpoint lies ~515 kb upstream of the *PVRL3* gene, while the chromosome 1 breakpoint lies ~50 kb upstream of the *NEK7* gene. Despite the fact that *NEK7* is closer to a translocation breakpoint than *PVRL3*, *NEK7* transcript levels are unaltered in patient DGAP113 lymphoblastoid cells and *Nek7*-deficient mice exhibit no detectable ocular phenotype. In contrast, the expression of *PVRL3*, which encodes the cell adhesion protein Nectin 3, is significantly reduced in patient DGAP113 lymphoblastoid cells, likely due to a position effect caused by the chromosomal translocation. Nectin 3 is expressed in the mouse embryonic ciliary body and lens. Moreover, *Pvrl3* knockout mice as well as a spontaneous mouse mutant *ari* (anterior retinal inversion), that maps to the *Pvrl3* locus, exhibit lens and other ocular defects involving the ciliary body. Collectively, these data identify *PVRL3* as a critical gene involved in a Nectin-mediated cell-cell adhesion mechanism in human ocular development.

Keywords

Cataract; Lens; *PVRL3*; Nectin; Cell-Adhesion; Ciliary Body

INTRODUCTION

Among ocular defects affecting humans, opacity in the ocular lens – clinically termed cataract – is classified as congenital or age-related and remains the leading cause of blindness, affecting approximately 25 million individuals worldwide (Graw 2009). Congenital cataract, although less common than age-related cataract, is responsible for one-tenth of all childhood blindness and occurs in isolation or in association with other defects of ocular development (Bermejo and Martinez-Frias 1998; Hejtmancik 2008; Jensen and Goldschmidt 1971). To date, isolated cataracts have been mapped to approximately 30 loci, of which more than 20 are associated with mutations in specific genes (Shiels and Hejtmancik 2007). Approximately half of these known mutations are in genes that encode crystallins (*CRYAA* [OMIM 123580], *CRYAB* [OMIM 123590], *CRYBB1* [OMIM 600929], *CRYBB2* [OMIM 123620], *CRYBB3* [OMIM 123630], *CRYBA1* [OMIM 123610], *CRYBA4* [OMIM 123631], *CRYGC* [OMIM 123680], and *CRYGD* [OMIM 1243690]), which are soluble proteins that are the major constituents of the vertebrate lens and play a role in maintaining lens transparency (Shiels and Hejtmancik 2007).

The remainder of the mutations are in functionally diverse genes which encode gap-junction connexin proteins (*GJA3* [MIM 121015], *GJA8* [OMIM 600897] (Mackay et al. 1999, Shiels et al. 1998)), a heat shock transcription factor (*HSF4* [OMIM 602438] (Bu et al. 2002)), homeodomain, bZIP and forkhead transcription factors (*PITX3* [OMIM 602669] (Semina et al. 1998), *MAF* [OMIM 177075] (Jamieson et al. 2002), *FOXO3* [OMIM 601094] (Semina et al. 2001)), an aquaporin (*MIP* [OMIM 154050] (Berry et al. 2000)), a membrane protein (*LIM2* [OMIM 154045] (Pras et al. 2002)), an ephrin receptor protein-tyrosine kinase (*EPHA2* [OMIM 176946] (Shiels et al. 2008)) and cytoskeletal proteins (*BFSP1* [OMIM 603307], (Ramachandran et al. 2007), *BSFP2* [OMIM 603212] (Conley et al. 2000)). In addition, mutations in the developmental regulatory factors *PAX6* ([OMIM 607108] (Glaser et al. 1994; Prosser et al. 1998)) and *EYAI* ([OMIM 601653] (Azuma et al. 2000)) have been found to cause congenital cataracts, along with other ocular defects.

One approach to gene discovery in congenital ocular defects is to study affected individuals who carry balanced chromosomal rearrangements. Both translocations and inversions can disrupt or de-regulate genes at either of the two chromosomal breakpoints that occur with these types of rearrangements (Lachke et al. 2011). The Developmental Genome Anatomy Project (DGAP) seeks to identify genes disrupted by chromosomal breakpoints that are causative for human birth defects (<http://dgap.pathology.org>; Higgins et al. 2008). One

individual, patient DGAP113, carried a t(1;3)(q31.3;q13.13) balanced translocation, severe bilateral congenital cataracts, mild developmental delay, an increased head circumference, and prominent extra-axial cerebrospinal fluid (CSF) spaces. This case thus afforded the opportunity to search for genes etiologic for the cataract phenotype. We sought definitive identification of the responsible gene(s) through an analysis of the expression of these genes in the subject's lymphoblastoid cells, and by analysis of the homologous mouse genes and the corresponding mouse mutants. We present data that *PVRL3* plays an important function in mammalian lens and ciliary body development, and that it represents the first Nectin family cell-cell adhesion protein associated with human ocular phenotype.

METHODS

Generation of Patient DGAP113 Cell Lines

All human study protocols were reviewed and approved by the Partners Health Care System Human Research Committee. Peripheral blood specimens were collected and lymphocyte cell transformation was performed using standard protocols (Bernacki et al. 2003) at the Massachusetts General Hospital Genomics Core Facility in the Center for Human Genetic Research (Boston, MA).

Cytogenetic Studies and Array CGH

The GTG-banded karyotype was evaluated at a resolution of 550 bands. Fluorescence *in situ* hybridization (FISH) probes used for mapping the breakpoints were derived from BACs selected from genomic analyses conducted with the University of California Santa Cruz (UCSC) Genome Browser and Database and the NCBI Human Genome Browser and Database. BACs from the RP1, RP3, RP4, RP5, RP6, RP11, and RP13 libraries were obtained from CHORI (Children's Hospital Oakland Research Institute, Oakland, CA). BACs from the CTB, CTC, and CTD libraries were obtained from Invitrogen (Carlsbad, CA). DNA was isolated using a standard protocol consisting of alkaline lysis, neutralization, and ethanol precipitation (Qiagen, Valencia, CA). Isolated DNA was labeled directly with either SpectrumGreen- or SpectrumOrange-conjugated dUTP, using the Nick Translation Reagent Kit from Abbott Molecular/Vysis (Des Plaines, IL), or indirectly with biotin or digoxigenin using the DIG DNA Labeling Kit or Biotin DNA Labeling Kit (Roche Diagnostics, Indianapolis, IN). Cot-I DNA was added to suppress repetitive sequences, and probes were ethanol precipitated and re-suspended in Hybrisol containing 50% formamide (Abbott Molecular/Vysis). FISH was performed as previously described (Higgins et al. 2008). Array-based comparative genomic hybridization (aCGH) experiments were performed using Spectral Genomics 2600 BAC arrays (Houston, TX) at an average resolution of ~1 Mb to exclude associated overt deletions and duplications.

Southern Blot Analysis and Breakpoint Cloning

Southern blotting was performed by standard methods (Southern, 1975). BAC RP11-401A10 DNA sequences overlapping the breakpoint critical region were examined using Repeat Masker to identify regions to generate specific probes. Genomic DNA probes ranging from ~250 to 500 base pairs (bp) were generated from non-repetitive sequences by PCR. PCR products were labeled with the Megaprime DNA labeling Kit (Amersham Biosciences, Piscataway, NJ). Aberrant bands detected in patient DGAP113 subject samples but absent in control samples localized the breakpoints to within these restriction fragments. Rearrangement breakpoints were cloned using modifications of the suppression PCR protocol (Siebert et al. 1995) as described (Alkuraya et al. 2006). Cloned junction fragments were sequenced using standard Sanger sequencing methods.

Immunofluorescence Microscopy

Mouse lens coronal sections for immunohistochemistry were prepared from mouse embryos fixed in 4% PFA on ice for 30 min, treated with 30% sucrose for 4 hr and embedded in OCT for cryosectioning. Chicken serum (Abcam) (5% solution in 1X PBS) was used for blocking and primary antibody incubation was done overnight at 4°C. Chick secondary antibodies used were conjugated with either Alexa 488 or Alexa 594 fluorophores (Invitrogen). Commercial antibodies were obtained from the following sources and used at 1:100 dilutions: Nectin 3 antibody [103-A1] (Abcam, ab16913), PVRL1 (Nectin 1) antibody (Abcam, ab66985), and I+S Afadin antibody (Abcam, ab11338), E-Cadherin (Abcam ab76055), ZO-1 (Invitrogen, 339100). To verify Nectin 3 antibody specificity, we analyzed Nectin 3 in the eye and found it correlated with the previously reported Nectin 3 expression pattern (Inagaki et al. 2005). All immunofluorescence experiments were performed with primary and secondary antibody only controls, which exhibited no detectable signal. Unless otherwise noted, all images were obtained by confocal microscopy using a Leica model TCS SP2 instrument with optical sections of 0.6–1.0 μm. Digitized images were processed with Adobe Photoshop.

Mouse Husbandry

All mice were treated in accordance with the protocols established by the Association for Research in Vision and Ophthalmology (ARVO). The Animal Care and Use Committees of Kobe University (Hyogo, Japan), Columbus Children's Research Institute (Columbus, OH) or Harvard Medical School (Boston, MA) approved all experimental protocols involving mutant mice and their controls. Wild type CD-1 outbred mice were obtained from Charles River Laboratories (Boston, MA) and used for immunohistochemical analyses. Mice were housed in a 14 h light to 10 h dark cycle, and mutant and littermate control mice were housed together to control for cage-dependent differences. The morning of vaginal plug discovery was taken as embryonic day E0.5. Mice used in this study were obtained from Kobe University, Miami University, Charles River Laboratories (Boston, MA), or from the laboratories of Dr. Y. Takai (Kobe University, Japan), Dr. M. Robinson (Miami University, OH), Dr. B. Motro (Bar-Ilan University, Israel) or Dr. R. Maas (Brigham and Women's Hospital and Harvard Medical School). Mice at all sites were regularly screened for pathogens. Two independent *Nek7* hypomorphic alleles were generated as gene trap insertions using mES cells obtained from BayGenomics Inc., and the Sanger Institute Gene Trap Resource (SIGTR). The targeted mES cells were subjected to blastocyst injection and germline competent chimeras were obtained and bred to achieve germline transmission. *Nek7* heterozygotes were initially crossed to generate *Nek7* homozygotes. Ocular phenotypic analyses were conducted using stereomicroscopy and histological sectioning. Degree of loss-of-function was analyzed by quantitative Reverse Transcriptase (qRT)-PCR. A third independently generated *Nek7* null allele was analyzed for the presence of a lens phenotype (Salem et al. 2010).

Microarray Analysis of Mouse Embryonic Lens

Total RNA was extracted from several hundred micro-dissected mouse embryonic day 11 lenses or whole embryonic tissue minus the eye region at stages E10.5 through E12.5 using the RNeasy Mini Kit (Qiagen). Standard Affymetrix protocols were used to prepare cDNA and biotin labeled cRNA using *in vitro* transcription. Microarray analysis was performed on biological triplicates by hybridization to the Affymetrix Mouse 430 2.0 chip in the Biopolymers facility at Harvard Medical School. Around 150 lenses were used per replicate and the data analyzed as described previously (Choe et al. 2005). The lens microarray analyses will be described in greater detail elsewhere.

RNA Analysis of Lymphoblastoid Cells

Total RNA was extracted from lymphoblastoid cell lines using the RNeasy Mini Kit (Qiagen). An iScript cDNA Synthesis Kit (Bio-Rad) was used followed by both regular PCR as well as quantitative PCR using an iQ SYBR green kit and analysis on a LightCycler (Bio-Rad). 5'-GAGTTCTAAAGTTCCTGTTGC-3' (NEK7-f5) and 5'-GAGGTATGACTTGACACAAAATA-3' (NEK7-r5) were used for amplification of a 1001 bp product specific to human *NEK7*. 5'-GTTACATCCCGCTTGAAA-3' (PVRL3-F) and 5'-CCCAGTCAATATGTGCAACG-3' (PVRL3-R) were used for amplification of a 169 bp product specific to human *PVRL3*. β -Actin was used as a housekeeping gene and was amplified by the primers 5'-AGCCTCGCCTTTGCCGA-3' (h-bActin-qF1) and 5'-CTGGTGCCTGGGCG-3' (h-bActin-qR1).

Genetic Mapping of the *ari* Mutation

Homozygous transgenic mice from line OVE401 that express FGF1 in the lens (Robinson et al., 1995) were maintained by brother-sister mating. After several generations of maintenance a litter of OVE401 pups contained several mice with microphthalmia. Outcrossing these microphthalmic pups with FVB/N inbred mice resulted in hemizygous transgenic litters with normal eye size, and intercrossing these F1 pups gave rise to microphthalmic offspring with a frequency of 25%; the transgene did not co-segregate with the microphthalmic phenotype. We determined that the microphthalmic phenotype was the result of an autosomal recessive mutation that spontaneously arose in the OVE401 transgenic mice, and named the mutation *ari* for anterior retinal inversion. The genetic location of the *ari* mutation was determined by a genetic screen using homozygous *ari* (non-transgenic) mice on an FVB/N background crossed to wild type C57BL/6 mice. All F1 mice were agouti and had normal eye size. F1 mice were backcrossed to homozygous FVB/N *ari* mice and the resultant backcross pups were collected for eye morphology and genomic DNA. Genomic DNA was tested for microsatellite polymorphisms between FVB/N and C57BL/6 and genotypes were compared with eye morphology to look for co-segregation and recombination between the microphthalmic phenotype and microsatellite polymorphisms. After an initial analysis of 24 backcross animals localized the *ari* mutation to mouse chromosome 16, we tested an additional 665 backcross progeny to localize the *ari* mutation to mouse chromosome 16 between D16Mit126 and D16Mit61.

In situ Hybridization Analysis of *Pvrl3* Expression

Pvrl3 expression was examined in wild type FVB/N and isogenic *ari* homozygous mutant mice by *in situ* hybridization. *In situ* hybridizations were carried out according to the methods described in Robinson et al., 1995. using an antisense riboprobe consisting of a *Pvrl3* retina EST clone (IMAGE 536340) labeled with ³⁵S-UTP. A *Pvrl3* sense riboprobe was used as a control, and exhibited no detectable signal. Sections were counterstained with hematoxylin and hybridization signals were viewed by dark field microscopy.

Analysis of *PVRL3* Upstream Region on Chromosome 3:q13.13

The chromosome 3 region upstream of *PVRL3* was analyzed using the University of California - Santa Cruz (UCSC) Genome Browser on Human Mar. 2006 (NCBI36/hg18) Assembly. Specifically, track settings for the ENCODE Enhancer- and Promoter-Associated Histone Mark (H3K4Me1) on 8 cell lines; the ENCODE Enhancer- and Promoter-Associated Histone Mark (H3K27Ac) on 8 cell lines; the ENCODE Enhancer- and Promoter-Associated Histone Mark (H3K4Me3) on 9 cell lines were used for analysis. This analysis indicated the presence of distinct loci in the *PVRL3* upstream region with a high mono-methylated histone H3 lysine 4 (H3K4Me1) and histone 3 lysine 4 acetylation (H3K27Ac) content, compared to tri-methylated histone H3 lysine 4 (H3K4Me3). Taken

with existing ChIP-Seq data for transcription factors in the same genomic region (Heintzman et al. 2007; Hon et al. 2008), this analysis suggests that the *PVRL3* upstream region may contain potential long-range control elements that regulate *Pvr13* expression.

RESULTS

Clinical Phenotype of Patient DGAP113

A male individual of Hispanic descent was enrolled in the study as patient DGAP113. He carried an apparently balanced chromosomal rearrangement, 46,XY,t(1;3)(q32.1;q13.2), and had severe bilateral congenital cataracts, mild developmental delay, and a head circumference greater than the 95th percentile. The cataracts were sufficiently severe that the physician was not comfortable in assigning them to a specific class/sub-type. No obvious defects in the ciliary body were noted. However, the ciliary epithelium can be potentially affected by decreased function of *PVRL3* (for details see sections on *PVRL3* mouse mutants). Because the ciliary epithelium is not easily observed in a standard ophthalmic exam, specialized techniques (*e.g.* use of high-resolution ultrasound) may be necessary to detect the presence of subtle abnormalities in cellular morphology or hypomorphic defects. Because such high-resolution techniques were not used at the time of the ocular exam of the patient, the presence of subtle defects in the ciliary epithelium (*e.g.* reduction in size or function) cannot be ruled out. A head MRI at about 6 months of age showed prominent bilateral frontal subarachnoid spaces that were interpreted as extra-axial CSF spaces, with normal morphology of the brain and ventricles. The orbits and sinuses appeared normal. There was no evidence of maternal rubella infection, or of other *in utero* or pregnancy complications, and there were no abnormal findings by ultrasound. Galactosemia and reducing substance tests were negative. No phenotype was observed in the parents. There was no consanguinity in this family. In addition, the parents' karyotypes were normal. Therefore, the phenotype was interpreted to result from a *de novo* genetic rearrangement.

Molecular and Cytogenetic Analysis of Patient DGAP113

Cytogenetic analysis of metaphase chromosomes from peripheral blood lymphocytes revealed the patient DGAP113's karyotype to be 46,XY,t(1;3)(q32.1;q13.2) (Fig. 1A,B). To refine the translocation breakpoints, FISH was performed on metaphase chromosomes with a series of labeled BAC clones that mapped to the reported cytogenetic breakpoint on chromosome 1. These experiments identified a clone, RP11-401a10, that demonstrated hybridization signals on the normal chromosome 1, der(1) and der(3), indicating that the chromosome 1 breakpoint lies within this clone (Fig. 1C). Clones that overlapped with RP11-401a10, namely, RP11-141e20 and CTD-2373e11, hybridized to der(1) and der(3) respectively, localizing the breakpoint within an 11.8 kb interval. Southern blot analysis, using PCR products generated from BAC RP11-401a10 as probes, further narrowed the breakpoint to an interval spanning 1397 bp (Fig. 1D,E).

Suppression PCR was then performed on der(1) and the junction fragment cloned (Fig. 2A). On chromosome 1, the breakpoint occurred within a LINE element approximately 50 kb upstream of the *NEK7* gene. The breakpoint occurred at nucleotide position 198076137 on chromosome 1, while it occurred at nucleotide position 110275770 on chromosome 3 in the human genome sequence GRCh37/hg19 assembly (February 2009). The location of the chromosome 3 breakpoint was similarly narrowed by FISH and regular PCR (data not shown). On chromosome 3 the breakpoint occurred within an LTR and was 515 kb upstream of the gene *PVRL3* (Fig. 1E). The rearrangement resulted in the breakpoint lying 1219 kb downstream of the gene *DPPA4* on der(3) and 174 kb downstream of the gene *LHX9* on der(1) (Fig. 1E, Fig. 2A). Localization of the breakpoints with molecular techniques led to a revision of the karyotype to 46,XY,t(1;3)(q31.3;q13.13). Array comparative genomic

hybridization (aCGH) was performed with DNA from the patient DGAP113's lymphoblastoid cell line with a BAC array at ~1 Mb resolution across the genome to ensure that there were no overt submicroscopic imbalances at other locations in the genome. This analysis detected no chromosomal gains or losses (data not shown) although point mutations or other genomic aberrations below the limit of resolution cannot be ruled out. Therefore, these analyses identified *NEK7*, *PVRL3*, *LHX9* and *DPPA4*, which are the closest genes flanking the two breakpoints, as potential candidate genes dysregulated in DGAP113.

***Pvrl3* and *Nek7* are Expressed in the Mouse Lens**

To determine whether any of the four candidate genes surrounding the breakpoints could be potentially involved in the pathogenesis of the patient DGAP113's cataract phenotype, we examined the expression of the homologous mouse genes in the developing mouse lens. We dissected lenses from mouse embryos at embryonic day E11.5, a key time point in lens morphogenesis, and performed gene expression analyses by microarray. Our gene expression analyses showed high expression of the genes *Nek7* and *Pvrl3* in E11.5 lens tissues (Fig. 2B). On the other hand, the genes *Lhx9* and *Dppa4* showed no detectable expression in the E11.5 lens (Fig. 2B). These gene expression analyses suggested that *PVRL3* and *NEK7*, which are proximate to the der(1) and der(3) breakpoints, respectively, warranted further investigation.

Reduced *PVRL3* Expression in Patient DGAP113 Lymphoblastoid Cells

We hypothesized that either of the two chromosomal breakpoints, or both, might exert a position effect on *NEK7* or *PVRL3* and dysregulate their expression in the subject. Position effects on gene expression are well documented in human disease, and have been previously identified as a cause of cataract (Kleinjan and van Heyningen 1998, 2005).

To test this possibility, we examined the expression of *NEK7* and *PVRL3* in DGAP113 lymphoblastoid cells. Reverse Transcriptase (RT)-PCR analysis indicated that *PVRL3* was down-regulated in patient DGAP113's lymphoblastoid cells compared to controls (Fig. 2C). In contrast, *NEK7* expression in patient DGAP113's lymphoblastoid cells remained unaltered compared to controls. Moreover, characterization of multiple mouse mutants with *Nek7* deficiency, including two independent hypomorphic alleles generated in this study, and an independently generated *Nek7* null allele, demonstrated the absence of cataract, although *Nek7* null homozygotes demonstrated a late embryonic or early post-natal lethal phenotype with growth retardation (Suppl. Fig. 1A–H; Suppl. Fig. 3; Salem et al. 2010). Next, to determine the extent to which *PVRL3* expression was altered by its translocation to der(1) breakpoint, we conducted a quantitative-RT-PCR analysis in subject and control lymphoblastoid cells and estimated that *PVRL3* transcripts were reduced to about 40% of control levels in patient DGAP113's lymphoblastoid cells whereas, again, *NEK7* transcript levels were unaffected (Fig. 2D). Exon and splice junction sequencing indicated the absence of intragenic mutations in *PVRL3* (data not shown). These results indicate that *PVRL3* expression is affected by the chromosomal rearrangement in patient DGAP113, likely by a position effect.

Lens Expressed Genes Encode Nectin 3-Interacting Proteins

To further examine the potential role of *PVRL3* in the developing lens, we tested whether genes that encode Nectin 3-interacting proteins, curated from the literature, are also expressed in the lens. We focused on four putative Nectin 3-interacting proteins. *PARD3* is essential for the polarized growth of cells and interacts via its PDZ domain with the carboxy terminal tail of Nectin 3 (Takekuni et al. 2003). *MLLT4* (myeloid/lymphoid or mixed-lineage leukemia translocated 4), orthologous to *Drosophila* Trithorax, encodes the actin filament-binding protein Afadin, which is known to interact with Nectin 3 (Reymond et al.

2000; Satoh-Horikawa et al. 2000; Takekuni et al. 2003), as well as with JAG1, which also functions in lens development (Le et al. 2009; Saravanamuthu et al. 2009). Nectin 1 and Nectin 2 are Nectin family members that function as Ca^{2+} -independent immunoglobulin-like cell-cell adhesion molecules; either interacts with Nectin 3 in heterophilic trans-interactions to establish adherens junctions (Satoh-Horikawa et al. 2000; Fabre et al. 2002; Takekuni et al. 2003).

We analyzed the E11.5 mouse embryo lens microarray database and found that all four genes are expressed in a significantly lens-enriched manner when compared to control whole embryonic tissues (Fig. 3). Thus, genes encoding proteins that interact with Nectin 3 and that can establish adherens junctions with Nectin 3 in other tissues are also expressed with *PVRL3* in the developing mouse lens.

Nectin 3 is Expressed in the Lens

To determine the spatio-temporal expression pattern of Nectin 3 and of Nectin 3-interacting proteins in the developing lens, we performed immunofluorescence microscopy (IFM) on murine embryonic lens sections at different stages. In lens development, cells of the anterior epithelium of the lens (AEL) exit the cell cycle at the lens equatorial zone (EZ) and differentiate into posterior fiber cells (PFC) (Fig. 4A) (Lachke and Maas 2010). In later stages, fiber cells elongate along the anterior-posterior axis, fill the lens vesicle (LV), and eventually contact the posterior AEL, in which E-cadherin maintains the AEL cellular phenotype (Pontoriero et al. 2009).

We first analyzed Nectin 3 expression in lens development. At E13.5, Nectin 3 was expressed in the AEL, and appeared to asymmetrically localize to the apical surface of anterior epithelial cells, which face the fiber cell compartment (Fig. 4B,B'). As lens development progresses, Nectin 3 immunoreactivity increases from equatorial to the anterior central AEL (Suppl. Fig. 2A,A'), and at E18.5, Nectin 3 was intensely expressed in the entire subset of AEL that contacted fiber cells (Fig. 4C, C'). At E13.5, Afadin (MLLT4) was present in the mouse AEL and co-localized with Nectin 3 (Fig. 4D,D'). The Afadin-Nectin 3 co-localization was even more striking at E18.5 (Fig. 4E, E'). At E13.5, Nectin 1 was present in fiber cells adjacent to the Nectin 3-expressing AEL cells (Fig. 4F,F'). Previously, Nectin 2 was reported in both AEL and fiber cells at E11.5 (Okabe et al. 2004). These results indicate that Nectin 3 and four of its potential interacting proteins are coordinately expressed in overlapping patterns during lens development.

Nectin 3 Exhibits Polarized Localization in the Anterior Epithelium of the Lens (AEL)

To determine whether Nectin 3 is expressed in the AEL or fiber cells we performed IFM. We analyzed E18.5 mouse lens sections using antibodies against Nectin 3 and the lens-epithelial-specific marker E-Cadherin (Fig. 5A–C, A'–C'). In addition, we also analyzed E18.5 lens sections using antibodies against Nectin 3 and the protein ZO-1 (Fig. 5D–F, D'–F'), which co-localizes in the anterior epithelium/fiber cell interface (Nguyen et al. 2005; Inagaki et al. 2005) and which we found to localize apical to Nectin 3 in epithelial cells. The intracellular E-Cadherin - Nectin 3 - ZO-1 expression domains were progressively ordered in AEL cells from basal to apical, respectively, conforming to the pattern observed in other epithelia. Location of the ZO-1 expression domain - apical relative to Nectin 3 - in the AEL confirms that Nectin 3 is expressed and localized within the AEL and/or the AEL-fiber cell interface.

Nectin 3 and Afadin Co-localize in Cerebral Ventricular Ependymal Epithelium

To test if Nectin 3 was also expressed in brain, we performed immunofluorescence microscopy on mouse embryonic brain tissues. At E13.5, Nectin 3 was expressed in the

epithelial (ependymal) cells lining the cerebral ventricles (Fig. 6A). Nectin 3 protein was localized near the apical surface that faces the ventricular lumen (Fig. 6A'). Afadin was also strongly expressed in a similar manner in the ventricular epithelium and substantially overlapped with Nectin 3 protein (Fig. 6B,B',C,C'). Thus, Nectin 3 and Afadin are co-expressed in a polarized manner at the apical surface of the epithelial ependymal cells lining the mouse cerebral ventricles. This finding may prove relevant to the bi-frontal subarachnoid space phenotype in patient DGAP113.

Lens and other Ocular Defects in *Pvrl3*-null mice

Previous characterization of *Pvrl3* null mutants revealed that Nectin 3 and Nectin 1 function via heterophilic trans-interactions to mediate apex-apex adhesion between pigmented and non-pigmented cell layers of the ciliary body epithelium (Inagaki et al. 2005). We further analyzed these *Pvrl3* null mutant mice to determine if they also exhibit a lens defect. At postnatal day P1, *Pvrl3* null mutant eyes exhibited microphthalmia and an absence of vitreous and aqueous humors, compared to littermate controls (Fig. 7A–C, F). In addition, in contrast to control lenses, *Pvrl3* null mutant lenses had small, slit-like separations in the central cortical fiber cells adjacent to the AEL (Fig. 7D, G). These small, slit-like separations were also present in the peripheral cortical region of fiber cells adjacent to the AEL (Fig. 7E, H). Thus, *Pvrl3* homozygous null mutants have microphthalmia and lens defects in the region where the AEL associates with fiber cells and where Nectin 3 and its potential interacting partners (Nectin 1 and 2) are expressed. In addition, in contrast to *Pvrl3* nullizygotes, *Pvrl3* heterozygous mice had no lens defects. Thus in the mouse, *Pvrl3* nullizygosity is required to phenocopy the proband's *PVRL3*-related lens cataract phenotype.

Cataracts and Other Ocular Defects in a Spontaneous Mouse Mutant at the *Pvrl3* Locus

To gain further insight into the role of *Pvrl3* in ocular development, we analyzed a spontaneous mouse ocular mutant, *ari* (anterior retinal inversion) that likely results from a regulatory mutation in *Pvrl3*. *ari* is an autosomal recessive microphthalmia mutant that arose in the transgenic mouse line OVE401 (Robinson et al., 1995). *ari* homozygotes, in the original FVB/N genetic background, manifest retinal inversion (the anterior retinal tip is folded backwards onto itself, giving an 'inverted' appearance), abnormal ciliary body morphogenesis, absent vitreous, and the development of bilateral cataracts (Fig. 8A–B'). An initial genome scan with 24 backcross animals ((FVB/N-*ari* × C57BL/6) × FVB/N-*ari*) localized the genetic position of the underlying mutation to mouse chromosome 16, segregating independently of the original OVE401 transgene. Further refinement of the genetic position of *ari*, based on an analysis of 656 backcross progeny, localized it to a 2.3 Mb region spanning from 422 kb upstream to 1.8 Mb downstream of the *Pvrl3* transcription unit (Suppl. Fig. 3A,B; Suppl. Table 1). However, sequencing of *Pvrl3* exons and splice junctions in *ari* mutants failed to detect an intragenic mutation (data not shown).

Next, we tested if *Pvrl3* expression in developing ocular tissues was affected as a result of the *ari* mutation. Section *in situ* analyses of E15.5 and P1 mouse eyes revealed that the *Pvrl3* expression domain in the prospective ciliary epithelia in *ari* homozygous mice was reduced to background levels (Fig. 8C–D'; Suppl. Fig. 4C–D'). Surprisingly, *Pvrl3* expression in the embryonic and postnatal lens of *ari* homozygotes appeared similar to wild type (data not shown). These results suggest the existence of distinctly regulated *Pvrl3* expression domains in different ocular tissues.

DISCUSSION

Association of Patient DGAP113 Ocular Phenotype with Reduced *PVRL3* Expression

Molecular analysis of patient DGAP113, a male child with a balanced translocation between chromosomes 1 and 3, suggested that the dysregulated expression of any of four candidate genes, *DPPA4*, *LHX9*, *NEK7* or *PVRL3*, alone or in combination, could be potentially responsible for the patient DGAP113's ocular and CNS phenotypes. The breakpoint on chromosome 3 lies about 1219 kb downstream of *DPPA4* and about 515 kb upstream of *PVRL3*, with the breakpoint on chromosome 1 about 174 kb downstream of *LHX9* and about 50 kb upstream of *NEK7*. Because none of these four genes were directly disrupted by either breakpoint, and because the proband's genome appeared otherwise intact by aCGH, we hypothesized that a position effect, by either or both breakpoints, on any of these genes, alone or in combination, most likely accounts for patient DGAP113's phenotype. Position effects that act upon human genes to cause disease, including cataract, are well documented, with distances ranging from 10 kb to 1.2 Mb (Kleinjan and van Heyningen 1998; 2005). Indeed, position effect dysregulation of genes important in eye development, including *PAX6*, *MAF*, and *FOXC1* (Lauderdale et al. 2000; Jamieson et al. 2002; Davies et al. 1999), and of genes important in brain development, such as *SHH* and *SIX3* (Roessler et al. 1997; Wallis et al. 1999), have been reported.

To test this hypothesis and to determine whether dysregulation of any of the four candidate genes played a role in patient DGAP113's phenotype, we analyzed the developmental expression of the homologous mouse genes. Both *Nek7* and *Pvrl3*, but not *Dpp4a* or *Lhx9*, were expressed in both the developing mouse lens and CNS. *Nek7* (Never in mitosis gene A-related Kinase 7) encodes a NIMA-related protein kinase that controls initiation of mitosis and is expressed in the CNS (Feige and Motro 2002; Kandli et al. 2000; Kimura and Okano 2001; O'Connell MJ et al. 2003; OMIM 606848). *Pvrl3* (Poliovirus Receptor-Like 3) encodes an immunoglobulin-like cell adhesion protein, Nectin 3, which interacts with the protein Afadin, and can establish adherens junctions in co-operation with cadherin-catenin molecules in epithelial cells (Reymond et al. 2000; Satoh-Horikawa et al. 2000; Ogita et al. 2010; OMIM 607147). Based on the expression pattern of these genes, we prepared and made use of existing mouse mutants for *Nek7* and *Pvrl3*. First, we obtained two mouse ES cell lines containing *Nek7* gene trap insertion alleles and used these to generate hypomorphic *Nek7* mutants. In addition, we analyzed a targeted *Nek7* null allele (Salem et al. 2010) and demonstrated no overt lens or ocular phenotype in hetero- or homozygotes at stage P5. Despite a clear reduction or absence in *Nek7* transcript or protein levels, these hypomorphic or null mutant mice did not exhibit any consistent homozygous phenotype. Moreover, *NEK7* expression was not significantly altered in patient DGAP113's lymphoblastoid cells lines compared to normal controls. Collectively, these results suggest that alterations in *NEK7* expression do not contribute significantly to the DGAP113 cataract phenotype.

In view of these findings, we hypothesized that *PVRL3* deficiency, as a result of a position effect engendered by patient DGAP113's translocation, was the most likely cause of patient DGAP113's cataract phenotype. Of note, patient DGAP113's translocation separates the *PVRL3* upstream genomic region, which is retained on der(3), from the *PVRL3* gene, which is translocated to der(1). Consistent with this, and in contrast to *NEK7*, *PVRL3* expression was reduced to approximately 40% of wild type levels in patient DGAP113's lymphoblastoid cells. In this context, the fact that *Pvrl3* heterozygous mice do not display a lens phenotype, whereas *Pvrl3* homozygotes do, is not unexpected because nullizygosity in mouse is frequently required to recapitulate a human haploinsufficiency phenotype (Lachke et al. 2011; Sandilands et al. 2003; Seidman and Seidman, 2002; White et al. 1998). However, because *Pvrl3* is expressed in multiple ocular tissues, these animals cannot address the question of an autonomous requirement for *Pvrl3* function in specific ocular

tissues. Moreover, the patient DGAP113 had severe bilateral cataracts but did not exhibit overt ciliary body defects. On the other hand, the *Pvrl3* null mouse mutants exhibit both lens and ciliary epithelial defects. The basis for this discrepancy may lie in the difference in the nature of the *Pvrl3* mutation between the mouse and the human. Alternately, the potential anatomic effects of defective ciliary epithelial function may differ between mice and humans. Nonetheless, the overall conclusion that reduced *Pvrl3* function in the eye results in a lens defect in the mouse and human is consistent with all mutant alleles studied, in both human and mouse.

Interestingly, analysis of the potential chromatin structure of the *PVRL3* upstream region in eight human cell lines, using the UCSC genome browser (see Methods), revealed the presence of potential long-range regulatory elements (Supp. Fig. 5). It is possible that separation of the *PVRL3* upstream region from the *PVRL3* transcription unit may separate lens-specific - but not ciliary body-specific - control elements, therefore accounting for the lack of obvious ciliary body phenotypes in the patient. For example, consistent with separate tissue-specific control elements, the *ari* mutant illustrates how *Pvrl3* expression in ciliary epithelia and lens can be de-coupled. In sum, *Pvrl3* expression in the developing mouse lens and CNS, and reduced expression of *PVRL3* in patient DGAP113 lymphoblastoid cells, support the view that reduced *PVRL3* expression contributes to in the ocular phenotype in patient DGAP113.

The Role of *Pvrl3* in Ocular Development and Cataract Formation

To obtain more definitive evidence for this hypothesis, we analyzed the ocular phenotype in two strains of *Pvrl3* loss-of-function mice. While patient DGAP113 also exhibits a CNS phenotype of prominent bi-frontal subarachnoid spaces, the developing lens constitutes a highly tractable system in which to ask questions about developmental mechanisms, due to its well-defined embryology and underlying gene regulatory network (GRN) (Donner et al. 2006; Lachke and Maas 2010).

In lens development, various cell adhesion molecules are dynamically expressed in both the AEL and fiber cell compartments (Beebe et al. 2001; Xu et al. 2002). Notably, differentiating fiber cells begin to elongate in the apical-basal axis and have distinct adherens junctions near their apical and basal surfaces (Beebe et al. 2001; Kuszak et al. 1995). Through their respective apical surfaces, fiber cells at this stage are in direct contact with the cells of the AEL. These contacts are lost as fiber cells cease to elongate, and this loss is associated with a loss of adherens complexes (Bassnett and Beebe, 2004). It is thus highly attractive to hypothesize that cell-adhesion proteins may function in these differentiation events.

The *PVRL* gene family encodes proteins termed Nectins that mediate cell-cell adhesion between similar or diverse epithelial cells through homophilic or heterophilic interactions, or through interaction with cadherins (Takai 2008a, b). Nectins show exclusive localization to adherens junctions (AJs) between neighboring cells, and are active in diverse cellular functions including cell movement, proliferation, survival, and differentiation (Barron et al. 2008; Mizoguchi et al. 2002; Ogita et al. 2008; 2010). Although E-cadherin and N-cadherin are expressed in the lens and are implicated in lens development, they can form only homophilic *trans*-interactions and thus may have their function largely restricted to cell-cell contacts between homologous cells. In contrast, because Nectins can form both homophilic or heterophilic *trans*-interactions and thus mediate cell-cell junctions in heterologous cells (e.g., AEL and fiber cells), they may have a function, non-overlapping and independent of cadherins, in the lens. Moreover, Nectin-mediated AJs are weaker than cadherin-mediated AJs, which may also reflect their utility in establishing cell-cell contacts that are necessarily temporary between migrating cells (fiber cells) and their stationary partners (AEL). Thus,

they comprise good candidates to mediate the cell-cell adhesion interactions essential to normal lens development.

For example, Nectin proteins also interact with Afadin, which itself binds to actin filaments. Afadin interacts with ZO-1, a tight junction component, which is expressed in the apical part of AEL, in the same region as Nectin 3 (Nielsen et al. 2003; Nguyen et al. 2005). It is tempting to speculate that Nectin 3 is involved in establishing adherens junctions between individual cells of the AEL, and also between cells of the AEL and migrating fiber cells. If so, *PVRL3* deficiency may lead to defects in cell adhesion in the AEL, or in the association of AEL and differentiating fiber cells. This may in turn disrupt fiber cell morphology, resulting in the formation of the slit-like separations in fiber cells that we observed, and culminating in cataract. This defect could also occur by reduced Nectin 3 interaction with other Nectin 3 interacting proteins such as PARD3, which interacts with CDC42 to generate cell polarity; CDC42 itself is implicated in lens epithelial invagination (Fig. 9A) (Chauhan et al. 2009). Reduced interactions between Nectin 3 and Nectin 1 or 2 proteins could also logically be expected to contribute to a cataract phenotype (Fig. 9B,C). Moreover, because heterophilic interactions of Nectin molecules can activate intracellular signaling, reduced Nectin 3 may also reduce signaling in the AEL or in fiber cells. Interestingly, in *ari* mutant mice, which exhibit cataracts, *Pvrl3* expression is reduced in the prospective ciliary epithelia but minimally affected in lens. This observation suggests that lens defects can be caused by *Pvrl3* deficiency in the ciliary epithelia. In the human patient however, ciliary body defects were not detected and the ocular orbits appeared normal - suggestive of normal ocular fluids. Together, these observations argue against an overt ciliary body-based aspect of *PVRL3* function as the primary pathogenic mechanism in the patient. An autonomous requirement for *Pvrl3* in the lens or the ciliary epithelium can only be conclusively addressed through the study of conditional null alleles in mice.

Lastly, a mechanism similar to that proposed in lens development involving defects in cell adhesion could also potentially account for the CNS phenotype in patient DGAP113. Nectin 3 is very specifically expressed in a polarized fashion long with Afadin at the apical surfaces of the ependymal cells that line the cerebral ventricles and subarachnoid space. The apical surfaces of ependymal cells are covered with the cilia and microvilli that are responsible for CSF circulation and resorption, respectively, and are also the site of tight junctions between adjacent ependymal cells. Defects at the apical surface of ependymal cells could ostensibly alter the dynamics of CSF resorption, and account for the expanded subarachnoid space phenotype in patient DGAP113.

In sum, we provide the first example of a nectin protein that is connected to human ocular disease. Data presented in this study lays the groundwork for further investigations into the function of Nectin 3 in ocular and CNS development, and into whether this function is indeed mediated through interactions with other proteins in ocular development, in particular in lens and ciliary body formation. Finally, it will be interesting to test if individuals with similar or overlapping phenotypes also have mutations in *PVRL3* or in its presumptive regulatory regions.

Supplementary Material

Refer to Web version on PubMed Central for supplementary material.

Acknowledgments

We thank the subject and his relatives for participating in the Developmental Genome Anatomy Project and Heather Ferguson, Chantal Kelly and Shahrin Ahsan for assistance as study coordinators. This work was supported by NIH grants 5R01EY10123-15 (RLM), 5R01HD060050-02 (RLM), 5P01GM061354-07 (CCM, RLM, JFG,

BJQ), R01EY021505 (SAL), R01EY12995 (MLR), and T35-EY07151 (QTD). All experiments comply with the current laws of the countries (U.S., Israel and Japan) in which they were performed.

REFERENCES

- Alkuraya FS, Saadi I, Lund JJ, Turbe-Doan A, Morton CC, Maas RL. SUMO1 haploinsufficiency leads to cleft lip and palate. *Science*. 2006; 313(5794):1751. [PubMed: 16990542]
- Azuma N, Hirakiyama A, Inoue T, Asaka A, Yamada M. Mutations of a human homologue of the *Drosophila* eyes absent gene (*EYA1*) detected in patients with congenital cataracts and ocular anterior segment anomalies. *Hum Mol Genet*. 2000; 9(3):363–366. [PubMed: 10655545]
- Barron MJ, Brookes SJ, Draper CE, Garrod D, Kirkham J, Shore RC, Dixon MJ. The cell adhesion molecule nectin-1 is critical for normal enamel formation in mice. *Hum Mol Genet*. 2008; 17:3509–3520. [PubMed: 18703497]
- Bassnett, S.; Beebe, D. Lens fiber differentiation. Chapter 9. In: Robinson, ML.; Lovicuo, F., editors. *Development of the ocular lens*. 2001. p. 214-244.
- Beebe DC, Vasiliev O, Guo J, Shui YB, Bassnett S. Changes in adhesion complexes define stages in the differentiation of lens fiber cells. *Invest Ophthalmol Vis Sci*. 2001; 42(3):727–734. [PubMed: 11222534]
- Bermejo E, Martinez-Frias ML. Congenital eye malformations: clinical-epidemiological analysis of 1,124,654 consecutive births in Spain. *Am J Med Genet*. 1998; 75(5):497–504. [PubMed: 9489793]
- Bernacki SH, Stankovic AK, Williams LO, Beck JC, Herndon JE, Snow-Bailey K, Prior TW, Matteson KJ, Wasserman LM, Cole EC, Stenzel TT. Establishment of stably EBV transformed cell lines from residual clinical blood samples for use in performance evaluation and quality assurance in molecular genetic testing. *J Mol Diagn*. 2003; 5(4):227–230. [PubMed: 14573781]
- Berry V, Francis P, Kaushal S, Moore A, Bhattacharya S. Missense mutations in MIP underlie autosomal dominant 'polymorphic' and lamellar cataracts linked to 12q. *Nat Genet*. 2000; 25(1):15–17. [PubMed: 10802646]
- Bu L, Jin Y, Shi Y, Chu R, Ban A, Eiberg H, Andres L, Jiang H, Zheng G, Qian M, Cui B, Xia Y, Liu J, Hu L, Zhao G, Hayden MR, Kong X. Mutant DNA-binding domain of HSF4 is associated with autosomal dominant lamellar and Marner cataract. *Nat Genet*. 2002; 31(3):276–278. [PubMed: 12089525]
- Chauhan BK, Disanza A, Choi SY, Faber SC, Lou M, Beggs HE, Scita G, Zheng Y, Lang RA. Cdc42- and IRSp53-dependent contractile filopodia tether presumptive lens and retina to coordinate epithelial invagination. *Development*. 2009; 136(21):3657–3667. [PubMed: 19820184]
- Choe SE, Boutros M, Michelson AM, Church GM, Halfon MS. Preferred analysis methods for Affymetrix GeneChips revealed by a wholly defined control dataset. *Genome Biol*. 2005; 6(2):R16. [PubMed: 15693945]
- Conley YP, Erturk D, Keverline A, Mah TS, Keravala A, Barnes LR, Bruchis A, Hess JF, FitzGerald PG, Weeks DE, Ferrell RE, Gorin MB. A juvenile-onset, progressive cataract locus on chromosome 3q21-q22 is associated with a missense mutation in the beaded filament structural protein-2. *Am J Hum Genet*. 2000; 66(4):1426–1431. [PubMed: 10729115]
- Davies AF, Mirza G, Flinter F, Ragoussis J. An interstitial deletion of 6p24-p25 proximal to the FKHL7 locus and including AP-2alpha that affects anterior eye chamber development. *J Med Genet*. 1999; 36(9):708–710. [PubMed: 10507730]
- Donner AL, Lachke SA, Maas RL. Lens induction in vertebrates: variations on a conserved theme of signaling events. *Semin Cell Dev Biol*. 2006; 17(6):676–685. [PubMed: 17164096]
- Fabre S, Reymond N, Cocchi F, Menotti L, Dubreuil P, Campadelli-Fiume G, Lopez M. Prominent role of the Ig-like V domain in trans-interactions of nectins. Nectin3 and nectin 4 bind to the predicted C-C'-C"-D beta-strands of the nectin1 V domain. *J Biol Chem*. 2002; 277(30):27006–27013. [PubMed: 12011057]
- Feige E, Motro B. The related murine kinases, Nek6 and Nek7, display distinct pattern of expression. *Mech Dev*. 2002; 110(1–2):219–223. [PubMed: 11744387]
- Glaser T, Jepeal L, Edwards JG, Young SR, Favor J, Maas RL. PAX6 gene dosage effect in a family with congenital cataracts, aniridia, anophthalmia and central nervous system defects. *Nat Genet*. 1994; 7(4):463–471. [PubMed: 7951315]

- Graw J. Mouse models of cataract. *J Genet.* 2009; 88(4):469–486. [PubMed: 20090208]
- Heintzman ND, Stuart RK, Hon G, Fu Y, et al. Distinct and predictive chromatin signatures of transcriptional promoters and enhancers in the human genome. *Nat Genet.* 2007; 39(3):311–318. [PubMed: 17277777]
- Hejtmancik JF. Congenital cataracts and their molecular genetics. *Sem Cell Dev Biol.* 2008; 19(2): 134–149.
- Higgins AW, Alkuraya FS, Bosco AF, Brown KK, Bruns GA, Donovan DJ, Eisenman R, Fan Y, Farra CG, Ferguson HL, Gusella JF, Harris DJ, Herrick SR, Kelly C, Kim HG, Kishikawa S, Korf BR, Kulkarni S, Lally E, Leach NT, Lemyre E, Lewis J, Ligon AH, Lu W, Maas RL, MacDonald ME, Moore SD, Peters RE, Quade BJ, Quintero-Rivera F, Saadi I, Shen Y, Shendure J, Williamson RE, Morton CC. Characterization of apparently balanced chromosomal rearrangements from the developmental genome anatomy project. *Am J Hum Genet.* 2008; 82(3):712–722. [PubMed: 18319076]
- Hon G, Ren B, Wang W. ChromaSig: a probabilistic approach to finding common chromatin signatures in the human genome. *PLoS Comput Biol.* 2008; 4(10) e1000201.
- Inagaki M, Irie K, Ishizaki H, Tanaka-Okamoto M, Morimoto K, Inoue E, Ohtsuka T, Miyoshi J, Takai Y. Roles of cell-adhesion molecules nectin 1 and nectin 3 in ciliary body development. *Development.* 2005; 132(7):1525–1537. [PubMed: 15728677]
- Inagaki M, Irie K, Ishizaki H, Tanaka-Okamoto M, Miyoshi J, Takai Y. Role of cell adhesion molecule nectin-3 in spermatid development. *Genes Cells.* 2006; 11(9):1125–1132. [PubMed: 16923130]
- Jamieson RV, Perveen R, Kerr B, Carette M, Yardley J, Heon E, Wirth MG, van Heyningen V, Donnai D, Munier F, Black GC. Domain disruption and mutation of the bZIP transcription factor, MAF, associated with cataract, ocular anterior segment dysgenesis and coloboma. *Hum Mol Genet.* 2002; 11(1):33–42. [PubMed: 11772997]
- Jensen S, Goldschmidt E. Genetic counselling in sporadic cases of congenital cataract. *Acta Ophthalmol (Copenh).* 1971; 49(4):572–576. [PubMed: 5171678]
- Kandli M, Feige E, Chen A, Kilfin G, Motro B. Isolation and characterization of two evolutionarily conserved murine kinases (Nek6 and nek7) related to the fungal mitotic regulator, NIMA. *Genomics.* 2000; 68(2):187–196. [PubMed: 10964517]
- Kimura M, Okano Y. Identification and assignment of the human NIMA-related protein kinase 7 gene (NEK7) to human chromosome 1q31.3. *Cytogenet Cell Genet.* 2001; 94(1–2):33–38. [PubMed: 11701951]
- Kleinjan DJ, van Heyningen V. Position effect in human genetic disease. *Hum Mol Genet.* 1998; 7(10):1611–1618. [PubMed: 9735382]
- Kleinjan DJ, van Heyningen V. Long-range control of gene expression: emerging mechanisms and disruption in disease. *Am J Hum Genet.* 2005; 76(1):8–32. [PubMed: 15549674]
- Kuszak JR, Novak LA, Brown HG. An ultrastructural analysis of the epithelial-fiber interface (EFI) in primate lenses. *Exp Eye Res.* 1995; 61(5):579–597. [PubMed: 8654501]
- Lachke SA, Maas RL. Building the developmental oculome: systems biology in vertebrate eye development and disease. *Wiley Inter Rev: Sys Biol Med.* 2010; 2(3):305–323.
- Lachke SA, Alkuraya FS, Kneeland S, Ohn T, Aboukhalil A, Howell G, Saadi I, Cavalleco R, Yingzi Y, Tsai AC, Nair SK, Cosma MI, Smith RS, Hodges E, AlFadhli SM, Al-Hajeri A, Shamseddin H, Behbehani A, Hannon G, Bulyk ML, Drack AV, Anderson PJ, John SW, Maas RL. Mutations in the RNA granule component TDRD7 cause cataract and glaucoma. *Science.* 2011; 331(6024): 1571–1576. [PubMed: 21436445]
- Lauderdale JD, Wilensky JS, Oliver ER, Walton DS, Glaser T. 3' deletions cause aniridia by preventing PAX6 gene expression. *Proc Natl Acad Sci USA.* 2000; 97(25):13755–13759. [PubMed: 11087823]
- Le TT, Conley KW, Brown NL. Jagged 1 is necessary for normal mouse lens formation. *Dev Biol.* 2009; 328(1):118–126. [PubMed: 19389370]
- Mackay D, Ionides A, Kibar Z, Rouleau G, Berry V, Moore A, Shiels A, Bhattacharya S. Connexin46 mutations in autosomal dominant congenital cataract. *Am J Hum Genet.* 1999; 64(5):1357–1364. [PubMed: 10205266]

- Mizoguchi A, Nakanishi H, Kimura K, Matsubara K, Ozaki-Kuroda K, Katata T, Honda T, Kiyohara Y, Heo K, Higashi M, Tsutsumi T, Sonoda S, Ide C, Takai Y. Nectin: an adhesion molecule involved in formation of synapses. *J Cell Biol.* 2002; 156(3):555–565. [PubMed: 11827984]
- Nguyen MM, Rivera C, Griep AE. Localization of PDZ domain containing proteins discs large-1 and scribble in the mouse eye. *Mol Vis.* 2005; 11:1183–1199. [PubMed: 16402019]
- Nielsen PA, Baruch A, Shestopalov VI, Giepmans BN, Dunia I, Benedetti EL, Kumar NM. Lens Connexins $\alpha 3\text{Cx}46$ and $\alpha 8\text{Cx}50$ Interact with Zonula Occludens Protein-1 (ZO-1). *Mol Biol Cell.* 2003; 14(6):2470–2481. [PubMed: 12808044]
- O'Connell MJ, Krien MJ, Hunter T. Never say never. The NIMA-related protein kinases in mitotic control. *Trends Cell Biol.* 2003; 13(5):221–228. [PubMed: 12742165]
- Ogita H, Takai Y. Cross-talk among integrin, cadherin, and growth factor receptor: roles of nectin and nectin-like molecule. *Int Rev Cytol.* 2008; 265:1–54. [PubMed: 18275885]
- Ogita H, Rikitake Y, Miyoshi J, Takai Y. Cell adhesion molecules nectins and associating proteins: Implications for physiology and pathology. *Proc Jpn Acad Ser B Phys Biol Sci.* 2010; 86(6):621–629.
- Okabe N, Ozaki-Kuroda K, Nakanishi H, Shimizu K, Takai Y. Expression patterns of nectins and afadin during epithelial remodeling in the mouse embryo. *Dev Dyn.* 2004; 230(1):174–186. [PubMed: 15108322]
- Pras E, Levy-Nissenbaum E, Bakhan T, Lahat H, Assia E, Geffen-Carmi N, Frydman M, Goldman B, Pras E. A missense mutation in the LIM2 gene is associated with autosomal recessive presenile cataract in an inbred Iraqi Jewish family. *Am J Hum Genet.* 2002; 70(5):1363–1367. [PubMed: 11917274]
- Pontoriero GF, Smith AN, Miller LA, Radice GL, West-Mays JA, Lang RA. Co-operative roles for E-cadherin and N-cadherin during lens vesicle separation and lens epithelial cell survival. *Dev Biol.* 2009; 326(2):403–417. [PubMed: 18996109]
- Prosser J, van Heyningen V. PAX6 mutations reviewed. *Hum Mutat.* 1998; 11(2):93–108. [PubMed: 9482572]
- Ramachandran RD, Perumalsamy V, Hejtmancik JF. Autosomal recessive juvenile onset cataract associated with mutation in BFSP1. *Hum Genet.* 2007; 121(3–4):475–482. [PubMed: 17225135]
- Reymond N, Borg J-P, Lecocq E, Adelaide J, Campadelli-Fiume G, Dubreuil P, Lopez M. Human nectin3/PRR3: a novel member of the PVR/PRR/nectin family that interacts with afadin. *Gene.* 2000; 255(2):347–355. [PubMed: 11024295]
- Robinson ML, Overbeek PA, Verran DJ, Grizzle WE, Stockard CR, Friesel R, Maciag T, Thompson JA. Extracellular FGF-1 acts as a lens differentiation factor in transgenic mice. *Development.* 1995; 121(2):505–514. [PubMed: 7539358]
- Roessler E, Ward DE, Gaudenz K, Belloni E, Scherer SW, Donnai D, Siegel-Bartelt J, Tsui LC, Muenke M. Cytogenetic rearrangements involving the loss of the Sonic Hedgehog gene at 7q36 cause holoprosencephaly. *Hum Genet.* 1997; 100(2):172–181. [PubMed: 9254845]
- Salem H, Rachmin I, Yissachar N, Cohen S, Amiel A, Haffner R, Lavi L, Motro B. Nek7 kinase targeting leads to early mortality, cytokinesis disturbance and polyploidy. *Oncogene.* 2010; 29(28):4046–4057. [PubMed: 20473324]
- Sandilands A, Prescott AR, Wegener A, Zoltoski RK, Hutcheson AM, Masaki S, Kuszak JR, Quinlan RA. Knockout of the intermediate filament protein CP49 destabilises the lens fibre cell cytoskeleton and decreases lens optical quality, but does not induce cataract. *Exp Eye Res.* 2003; 76(3):385–391. [PubMed: 12573667]
- Saravanamuthu SS, Gao CY, Zelenka PS. Notch signaling is required for lateral induction of Jagged1 during FGF-induced lens fiber differentiation. *Dev Biol.* 2009; 332(1):166–176. [PubMed: 19481073]
- Satoh-Horikawa K, Nakanishi H, Takahashi K, Miyahara M, Nishimura M, Tachibana K, Mizoguchi A, Takai Y. Nectin-3, a new member of immunoglobulin-like cell adhesion molecules that shows homophilic and heterophilic cell-cell adhesion activities. *J Biol Chem.* 2000; 275(14):10291–10299. [PubMed: 10744716]

- Semina EV, Brownell I, Mintz-Hittner HA, Murray JC, Jamrich M. Mutations in the human forkhead transcription factor FOXE3 associated with anterior segment ocular dysgenesis and cataracts. *Hum Mol Genet.* 2001; 10(3):231–236. [PubMed: 11159941]
- Semina EV, Ferrell RE, Mintz-Hittner HA, Bitoun P, Alward WL, Reiter RS, Funkhauser C, Daack-Hirsch S, Murray JC. A novel homeobox gene PITX3 is mutated in families with autosomal-dominant cataracts and ASMD. *Nat Genet.* 1998; 19(2):167–170. [PubMed: 9620774]
- Shiels A, Mackay D, Ionides A, Berry V, Moore A, Bhattacharya S. A missense mutation in the human connexin50 gene (GJA8) underlies autosomal dominant "zonular pulverulent" cataract, on chromosome 1q. *Am J Hum Genet.* 1998; 62(3):526–532. [PubMed: 9497259]
- Shiels A, Hejtmancik JF. Genetic origins of cataract. *Arch Ophthalmol.* 2007; 125(2):165–173. [PubMed: 17296892]
- Shiels A, Bennett TM, Knopf HL, Maraini G, Li A, Jiao X, Hejtmancik JF. The EPHA2 gene is associated with cataracts linked to chromosome 1p. *Mol Vis.* 2008; 14:2042–2055. [PubMed: 19005574]
- Siebert PD, Chenchik A, Kellogg DE, Lukyanov KA, Lukyanov SA. An improved PCR method for walking in uncloned genomic DNA. *Nuc Acids Res.* 1995; 23(6):1087–1088.
- Seidman JG, Seidman C. Transcription factor haploinsufficiency: when half a loaf is not enough. *J Clin Invest.* 2002; 109(4):451–455. [PubMed: 11854316]
- Southern EM. Detection of specific sequences among DNA fragments separated by gel electrophoresis. *J Mol Biol.* 1975; 98(3):503–517. [PubMed: 1195397]
- Takai Y, Ikeda W, Ogita H, Rikitake Y. The immunoglobulin-like cell adhesion molecule nectin and its associated protein afadin. *Annu Rev Cell Dev Biol.* 2008a; 24:309–342. [PubMed: 18593353]
- Takai Y, Miyoshi J, Ikeda W, Ogita H. Nectins and nectin-like molecules: roles in contact inhibition of cell movement and proliferation. *Nat Rev Mol Cell Biol.* 2008b; 9(8):603–615. [PubMed: 18648374]
- Takekuni K, Ikeda W, Fujito T, Morimoto K, Takeuchi M, Monden M, Takai Y. Direct binding of cell polarity protein PAR-3 to cell-cell adhesion molecule nectin at neuroepithelial cells of developing mouse. *J Biol Chem.* 2003; 278(8):5497–5500. 2003. [PubMed: 12515806]
- Wallis DE, Roessler E, Hehr U, Nanni L, Wiltshire T, Richieri-Costa A, Gillessen-Kaesbach G, Zackai EH, Rommens J, Muenke M. Mutations in the homeodomain of the human SIX3 gene cause holoprosencephaly. *Nat Genet.* 1999; 22(2):196–198. [PubMed: 10369266]
- White TW, Goodenough DA, Paul DL. Targeted ablation of connexin50 in mice results in microphthalmia and zonular pulverulent cataracts. *J Cell Biol.* 1998; 143:815–825. [PubMed: 9813099]
- Xu L, Overbeek PA, Reneker LA. Systematic Analysis of E-, N- and P-cadherin Expression in Mouse Eye Development. *Exp Eye Res.* 2002; 74(6):753–760. [PubMed: 12126948]

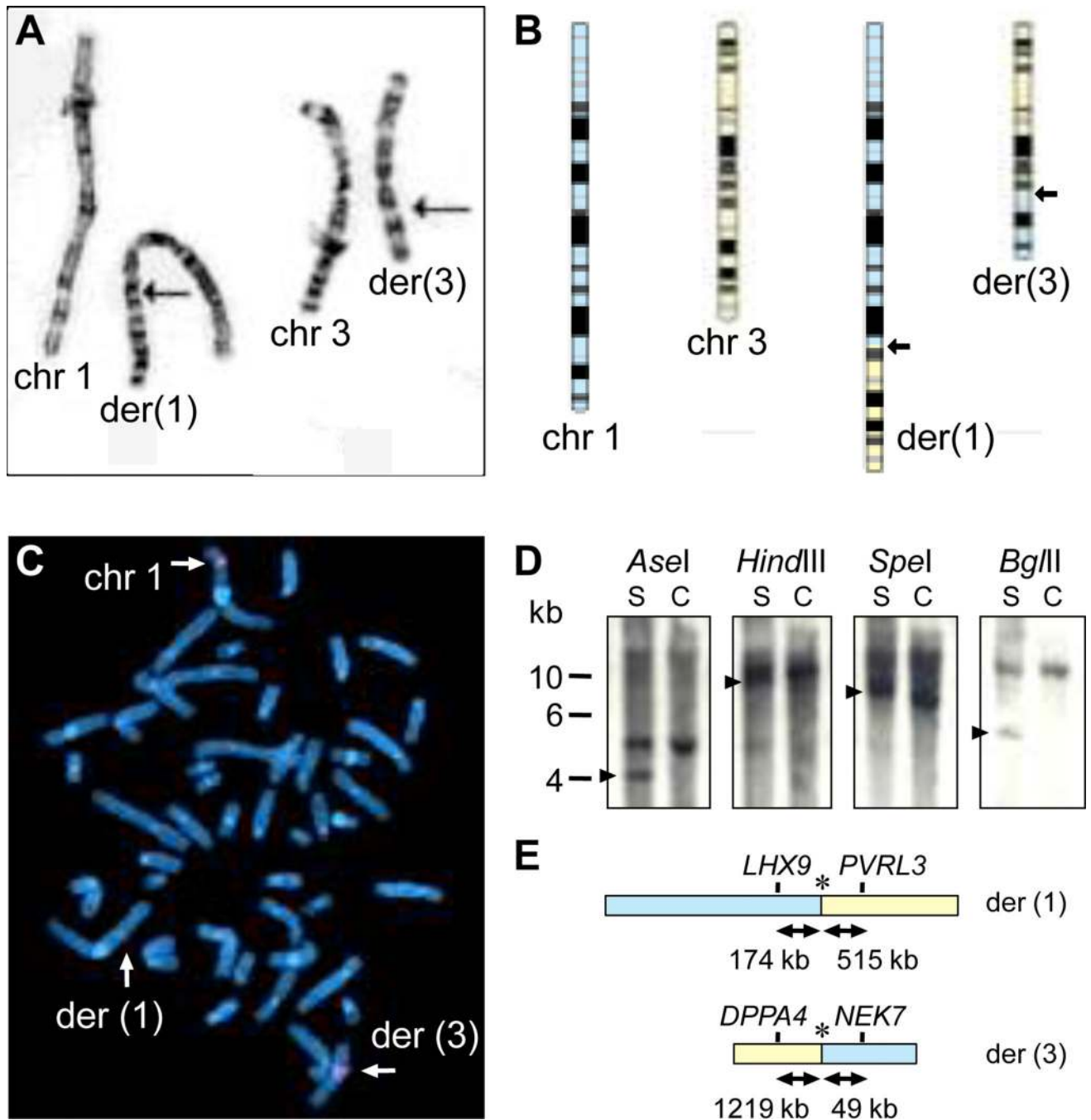


Fig. 1. Patient DGAP113 carries a balanced translocation between chromosomes 1 and 3. **(A)** GTG banded chromosomes of patient DGAP113. Arrows point to breakpoints on the derivative chromosomes. **(B)** Ideograms for chromosomes 1 and 3, and derivatives (der) 1 and 3. The derivatives represent the reported $t(1;3)(q32.1;13.2)$ in patient DGAP113. Arrows point to breakpoints on the derivative chromosomes. **(C)** Hybridization of BAC RP11-401a10 to metaphase chromosomes reveals signals (arrows) on chromosome 1, der(1) and der(3), indicating the breakpoint on chromosome 1 lies within this genomic clone. **(D)** Southern blot analysis of patient DGAP113 (subject, S) and control (C) DNAs. Enzymes used are indicated at top. The probe was a PCR product generated from BAC RP11-401a10.

Arrowheads indicate aberrant bands in the DGAP113 lane (S) indicating the break occurs within the region probed. Fragment sizes are from a DNA ladder. (E) Schematic representation of the rearranged loci as a result of the balanced translocation. Asterisk indicates breakpoint.

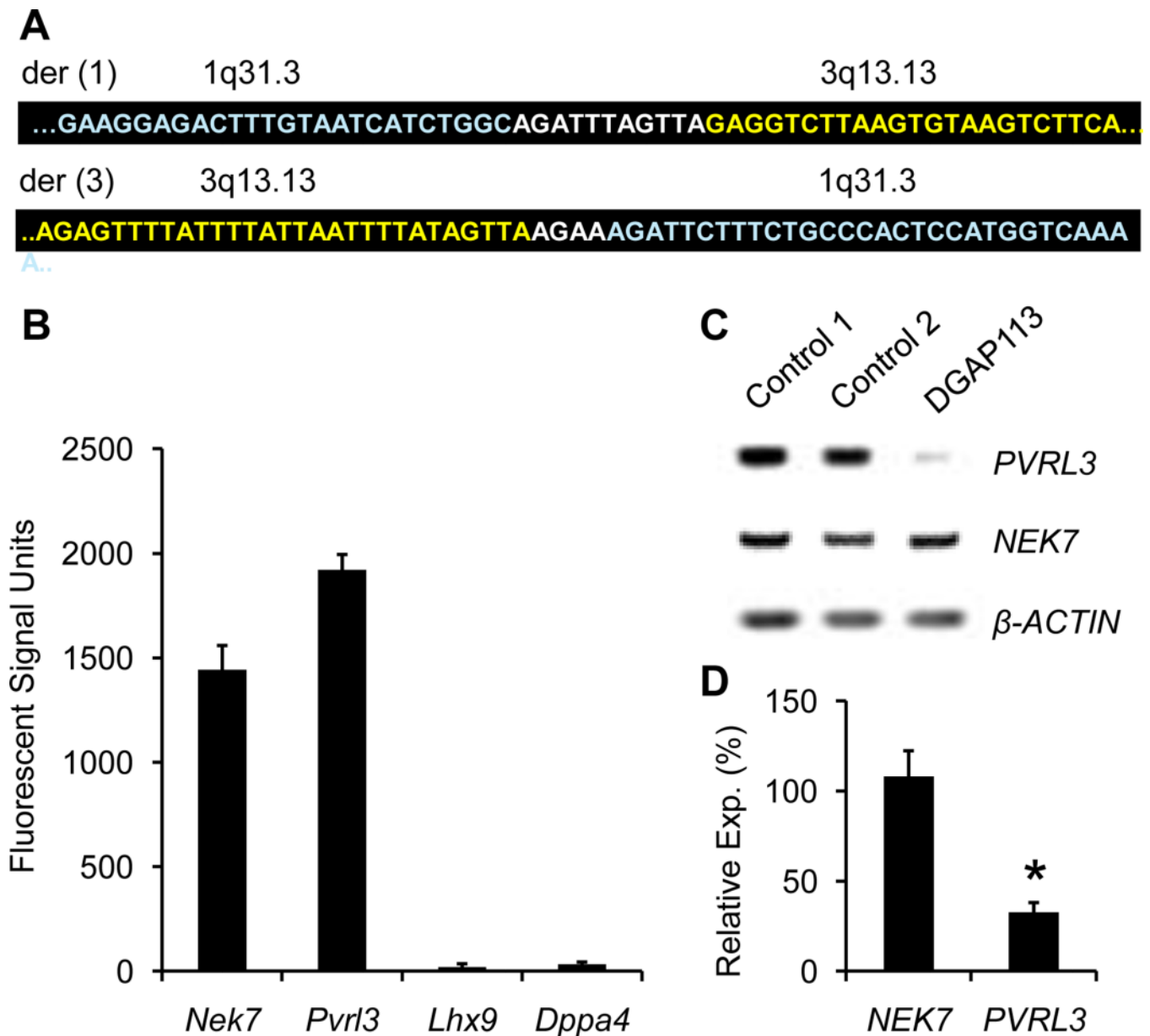


Fig. 2. Patient DGAP113 breakpoint resolution and reduced *PVRL3* expression. **(A)** Sequence at the breakpoint is shown with an 11 bp insertion in the der(1) and an 4 bp insertion in the der(3) (inserted nucleotides are shown in white text). **(B)** Expression of mouse *Nek7*, *Pvrl3*, *Lhx9* and *Dppa4* genes in E11.5 mouse embryonic lens assayed by fluorescence signal intensity from individual microarray probes specific for each transcript. **(C)** RT-PCR analysis of *PVRL3* and *NEK7* transcripts in lymphoblastoid cells from patient DGAP113 and two control subjects. Control is indicated by β -*ACTIN*. **(D)** Quantitative RT-PCR analysis reveals that *PVRL3* transcripts in patient DGAP113's lymphoblastoid cells are reduced to ~40% of levels in control lymphoblastoid cells (defined as 100%), while *NEK7* transcripts levels show no significant change. Asterisk indicates $p < 0.05$.

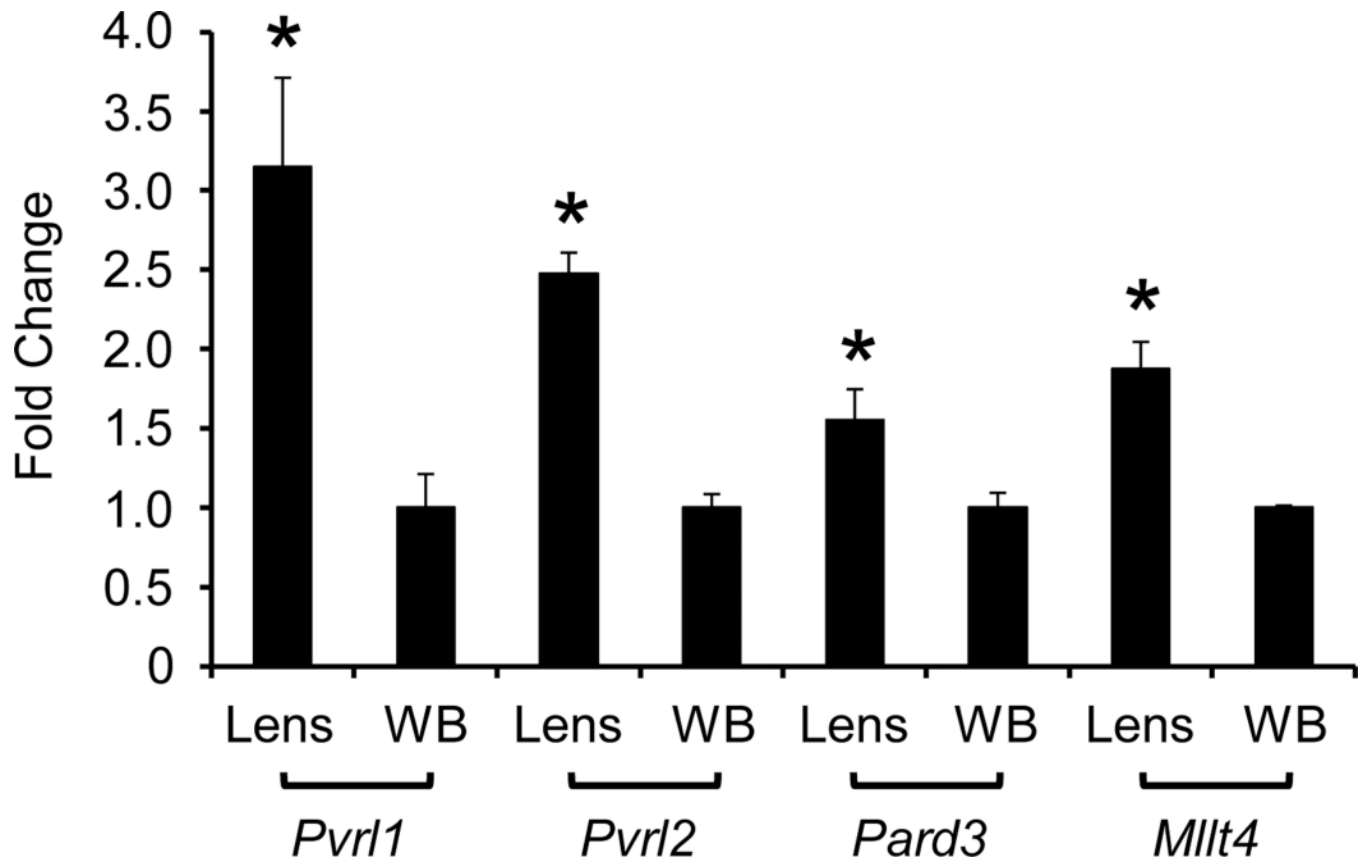


Fig. 3. Transcripts encoding Nectin 3-interacting proteins are enriched in the developing mouse lens. Fold changes estimated from fluorescence signal intensity from individual microarray probes specific for each of the genes *Pvr11*, *Pvr12*, *Pard3* and *Mllt4* indicate enriched expression in mouse E11.5 lens compared to whole embryonic tissue. Signal from whole body (WB) embryonic tissue was normalized for each transcript to represent 1.0-fold expression. Asterisk indicates $p < 0.05$.

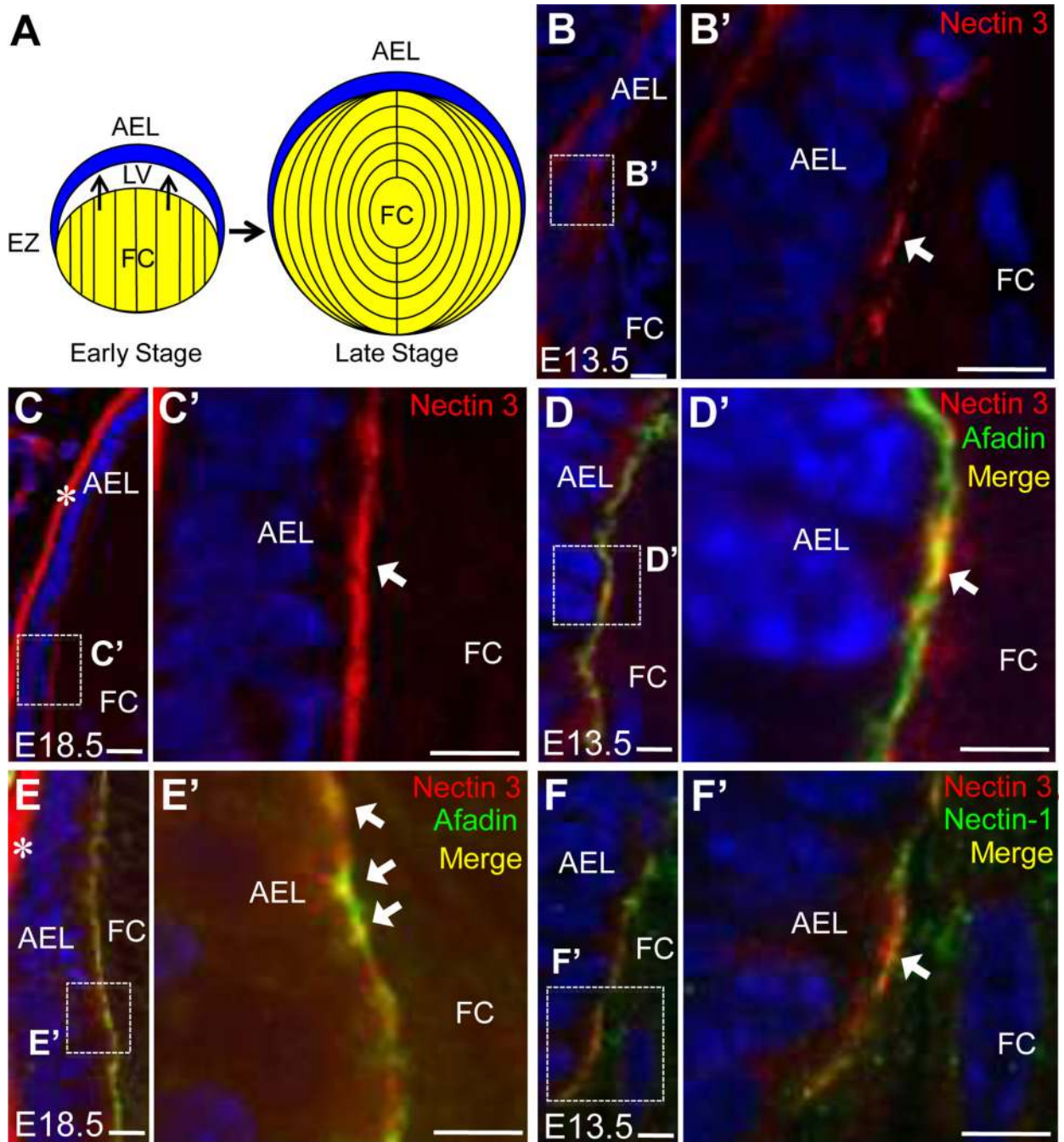


Fig. 4. Nectin 3 is expressed in the lens. **(A)** Schematic of early (left) and late (right) stages in lens development. Early stage depicts the lens vesicle (LV) stage when anterior epithelial cells of the lens (AEL, blue) exit the cell cycle in the equatorial zone (EZ) and differentiate into primary fiber cells (FC, yellow) in the posterior lens. At a later stage, fiber cells (FC, yellow) elongate, fill the LV cavity, and contact the apical surface of the AEL. In the central lens, fully mature fiber cells form “sutures” at their apical and basal surfaces, indicated by black vertical lines. **(B)** Immunofluorescence microscopy (IFM) of E13.5 mouse lens demonstrates Nectin 3 expression (red) in the AEL, being stronger near the transition zone. **(B')** High magnification of boxed region in (B). Polarized Nectin 3 expression at the apical

surface of the AEL (arrow). **(C)** IFM of E18.5 mouse lens demonstrates strong Nectin 3 expression (red) in the entire AEL. **(C')** High magnification of boxed region in (C). Polarized Nectin 3 expression at the apical surface of the AEL (arrow). **(D)** IFM of E13.5 mouse lens demonstrates Nectin 3 (red) and Afadin (green) expression. **(D')** High magnification of boxed region in (D). Polarized Nectin 3 (red) and Afadin (green) expression in the AEL (arrows). Co-localization is yellow. **(E)** IF of E18.5 mouse lens demonstrates Nectin 3 (red) and Afadin (green) expression. **(E')** High magnification of boxed region in (E). Polarized Nectin 3 (red) and Afadin (green) expression (arrow). Co-localization is yellow. **(F-F')** IFM of E13.5 lens indicates Nectin 1 expression in fiber cell compartment. **(F)** Nectin 3 (red) is expressed in AEL, Nectin 1 (green) in FCs. **(F')** High magnification of boxed region in (F). At high magnification, co-localization between Nectin 1 and 3 is detected (yellow, arrow). Abbr.: AEL, Anterior epithelium of the lens; FC, Fiber cells. Asterisk denotes non-specific staining of the lens capsule. Scale bars: (B) and (B') 15 μm , (C) 25 μm , (C') 7 μm , (D) 5 μm , (D') 4 μm , (E) 10 μm , (E') 5 μm .

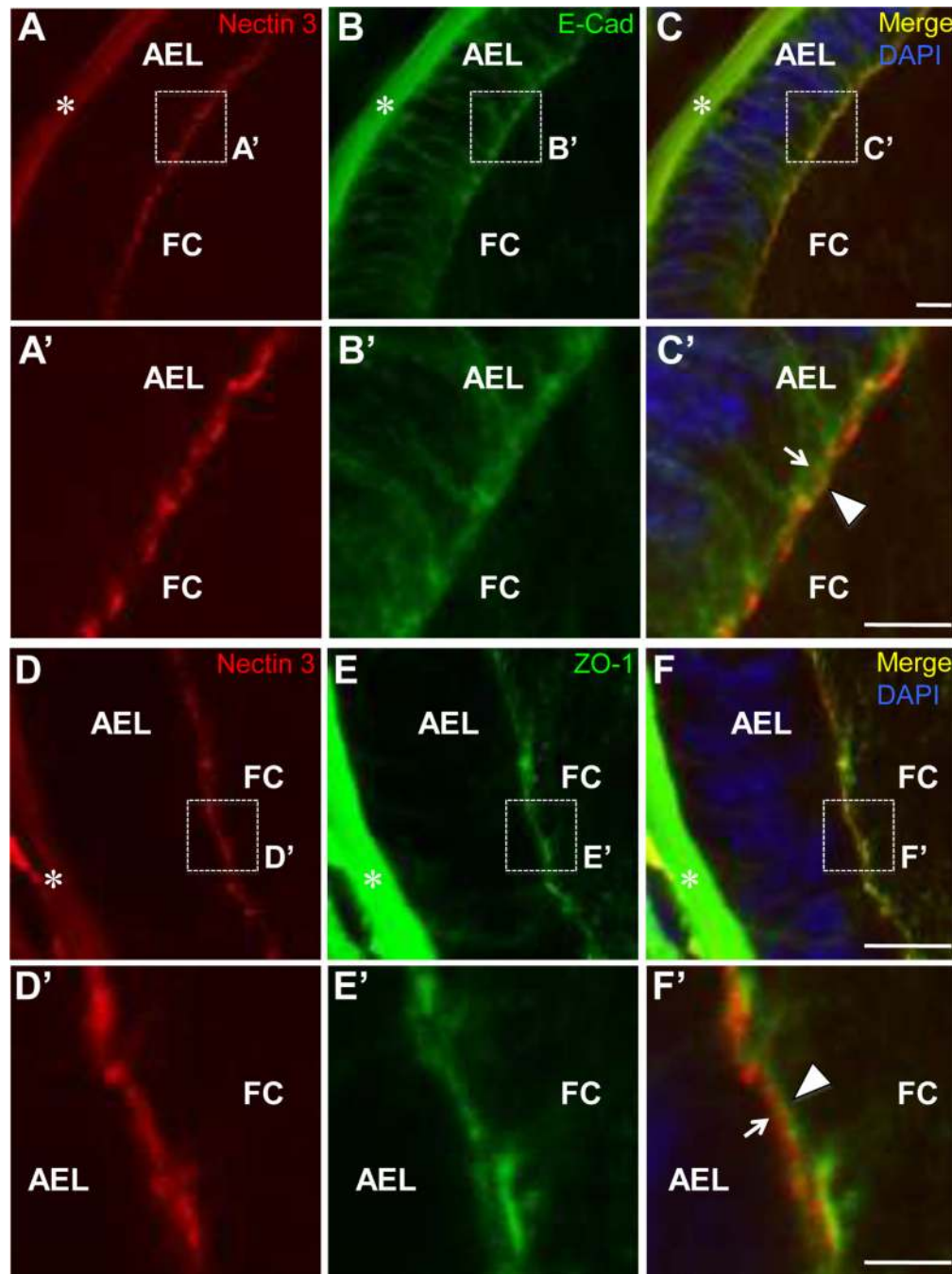


Fig. 5. Nectin 3 is expressed in anterior epithelium of the lens (AEL). **(A)** IFM analysis of E18.5 mouse lens demonstrates Nectin 3 expression (red) in the AEL. **(A')** High magnification of boxed region in (A). **(B)** IFM analysis of the same lens section, stained with E-Cadherin (green) in the AEL. **(B')** High magnification of boxed region in (B). **(C)** Merged image from (A) and (B). **(C')** High magnification of boxed region in (C) demonstrates that Nectin 3 expression localizes (arrowhead) apically with respect to E-Cadherin expression (arrow). Co-localization is yellow. **(D)** IFM analysis of E18.5 mouse lens demonstrates Nectin 3 expression (red) in the AEL. **(D')** High magnification of boxed region in (D). **(E)** IFM analysis of the same lens section stained with ZO-1 (green) in the AEL. **(E')** High

magnification of boxed region in (E). (F) Merged image from (D) and (E). (F') High magnification of boxed region in (F) demonstrates that Nectin 3 localizes (arrow) largely basally to ZO-1 expression (arrowhead). Co-localization is yellow. Abbr.: AEL, Anterior epithelium of the lens; FC, Fiber cells. Asterisk denotes non-specific staining of the lens capsule. Scale bars: (C) 4 μm , (C') 7 μm , (F) 10 μm , (F') 4 μm .

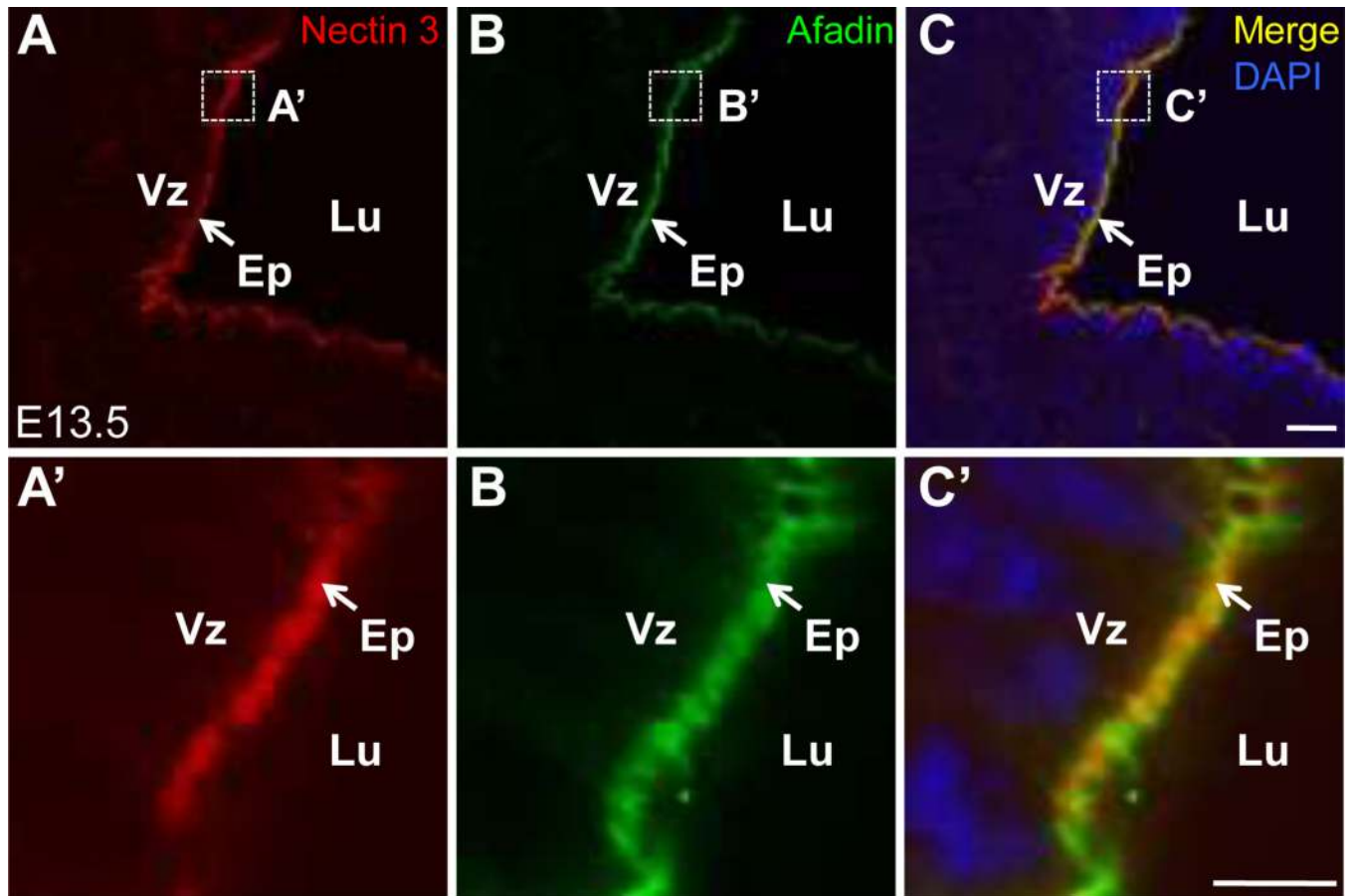


Fig. 6. Nectin 3 shows polarized localization in ventricular epithelium. **(A)** IFM analysis of E13.5 mouse brain demonstrates Nectin 3 expression in the epithelial cells lining of the ventricles. **(B)** These cells also express the actin filament-binding protein Afadin. **(C)** Co-localization of Nectin 3 and Afadin. **(A'–C')** High magnification of regions in (A–C). Abbr.: Ep, Ependyma; Lu, Lumen; Vz, Ventricular zone. Scale bars: (A–C) 40 μ m, (A'–C') 4 μ m.

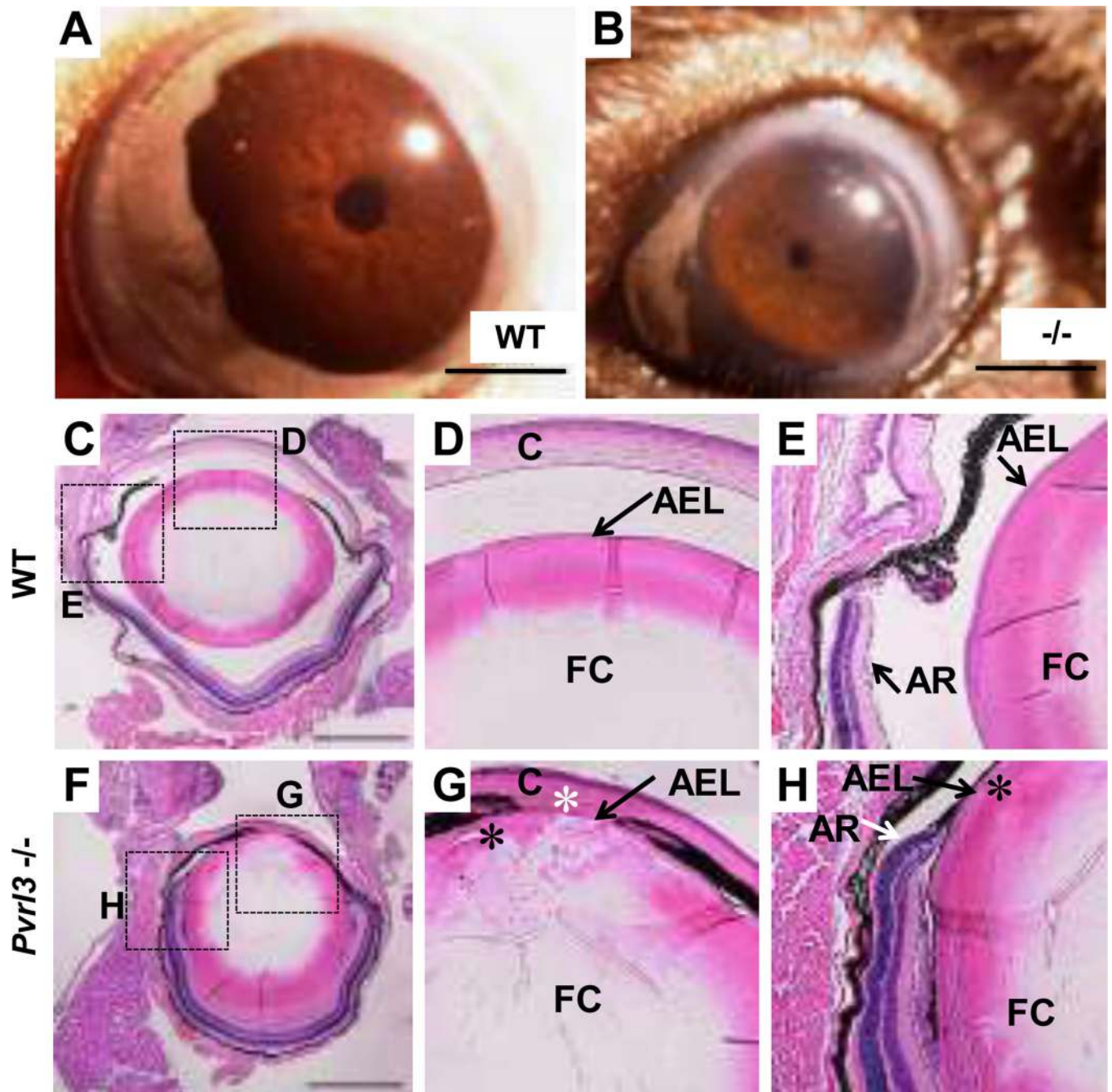


Fig. 7. *Pvr13* null mouse mutant exhibits lens and multiple ocular defects. **(A)** Eye of wild type (WT) 6 wk old mouse. **(B)** Eye of aged-matched *Pvr13* null 6 wk old mouse ($-/-$) that exhibits microphthalmia. **(C)** H&E stained coronal section of P1 wild type (WT) mouse eye. **(D)** High magnification of **(C)** showing region between lens AEL and FC compartments. **(E)** High magnification of **(C)** showing region between lens and anterior retina. **(F)** H&E stained coronal section of P1 *Pvr13* homozygous knockout mouse eye (*Pvr13* $-/-$). **(G)** High magnification of **(F)** showing lens region between AEL and FCs. Note the presence of small slit-like separations in FCs (black asterisk) and disruption of fiber cell morphology, hallmarks of certain types of cataract. Also note severe reduction of the anterior chamber

(white asterisk), normally present between the cornea and AEL. Also note the presence of eosinophilic material in the anterior chamber and the vitreous chamber in *Pvr13* $-/-$ mutants. **(H)** High magnification of (F) showing region between lens and anterior retina. Note small slit-like separations between AEL and FCs (black asterisk). Abbr.: AEL, Anterior epithelium of the lens; AR, Anterior retina; C, Cornea; FC, Fiber cells. Scale bar: 1mm.

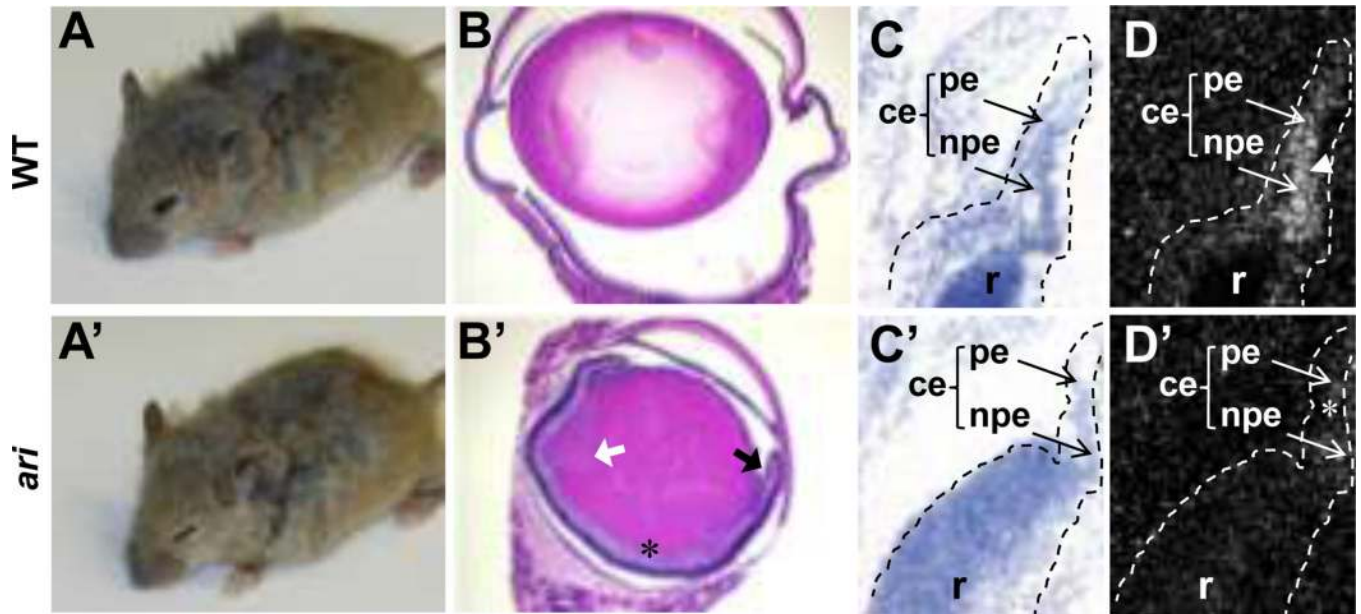


Fig. 8. *ari* homozygous mouse mutants exhibit cataracts and multiple ocular defects. (A) Wild type littermate with normal size eye (WT). (A') *ari/ari* homozygous mutant mice with microphthalmia. Both (A) and (A') are from ((FVB/N-*ari* × C57BL/6) × FVB/N-*ari*) backcross progeny. (B) H&E stained section of P27 wild type eye. (B') H&E stained section of P27 *ari/ari* mutant eye (FVB/N background) demonstrates anterior retinal inversion (black arrow), lack of vitreous (asterisk), and a defect in lens fiber cells (white arrow). (C) Hematoxylin stained section demonstrates morphology and (D) section *in situ* analysis of E15.5 wild type mouse demonstrates normal *Pvr13* expression (arrow) in the prospective ciliary epithelia (ce), which consists of both pigmented epithelium (pe) and non-pigmented epithelium (npe) (darkfield image). (C') Hematoxylin stained section demonstrates aberrant morphology and (D') section *in situ* analysis on the retinal margin of a P1 *ari* mouse mutant demonstrates reduced *Pvr13* expression (asterisk) in the prospective ciliary epithelia. The retina region including the developing ciliary body is outlined by the dashed line, with retinal pigment epithelium indicated by a black arrow. Abbr.: ce, prospective ciliary epithelium; npe, non-pigment epithelium; pe, pigment epithelium; r, retina.

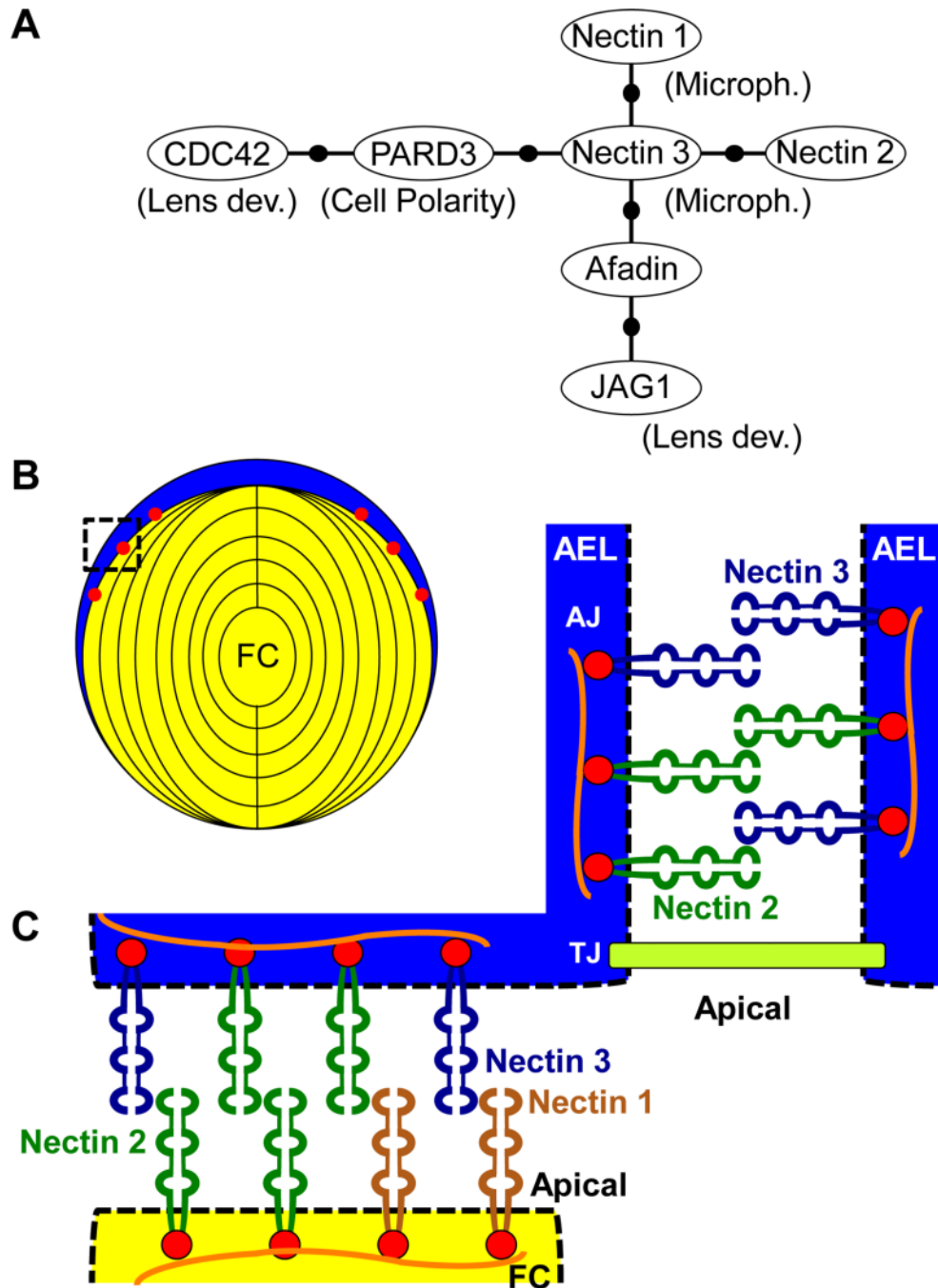


Fig. 9. Model for Nectin 3 function in the lens. **(A)** Protein interaction map of Nectin 3 and its known interacting partners, demonstrated to be expressed in the developing lens. Lines with black dots indicate direct interaction between proteins. Nectin 3 directly interacts with proteins that also function in lens development; mutations in some cause microphthalmia, lens and other ocular defects in mice. Abbr.: Lens dev., lens development; Microph, microphthalmia. **(B–D)** Model for how reduced *PVRL3* expression may cause cataract formation. **(B)** The lens is composed of cells of the AEL (blue) that differentiate into fiber cells (yellow) in the posterior lens. Fiber cells in the process of elongation are apposed to cells of the AEL at their apical surfaces and come in direct contact with them through

adhesive molecules (red). As these elongating fiber cells migrate to the central part of the lens, there is a rearrangement of adhesive molecules in mature fiber cells, which fuse at their anterior and basal surfaces with fiber cells from opposing ends to form sutures. Region of the anterior lens is highlighted by dashed black line in (C). (C) Nectin 3 protein is localized at the apical surface of the AEL and faces the apical surface of elongating FCs. Nectin 2 is also expressed in the AEL. Nectin 1 and 2 proteins localize to the apical surface of elongating FCs. Homo or heterophilic interactions between these molecules function to establish adherens junctions between individual cells of the AEL (Nectin 3-Nectin 3 or Nectin 3-Nectin 2 interactions), or between individual cells of the AEL and elongating FCs (Nectin 3-Nectin 2, Nectin 3-Nectin 1, Nectin 1-Nectin 2, Nectin 2-Nectin 2 interactions). Inside the cell, Nectin proteins interact with Afadin molecules (red circles) which themselves bind to F-actin (orange lines). Reduced *PVRL3* expression in the AEL leads to a reduction in AEL-FC association, formation of slit-like separations and culminating in cataract formation. The model shown does not preclude an additional contribution to the lens phenotype from Nectin 3 expression in the ciliary epithelium. Abbr.: AEL, Anterior epithelium of the lens; FCs, Fiber cells; AJ, adherens junction; TJ, tight junction.